IGOR GUSTAVO DA FONSECA CARRASQUEIRA

The Indian summer monsoon and the South American summer monsoon and their responses to different forcings in some key periods of the Neogene

Sao Paulo

2023

Resumo

Carrasqueira, I.G.F. A monção de verão indiana e a monção de verão sul-americana e suas respostas a diferentes forçantes em alguns períodos-chave do Neógeno. 2023. Tese Doutorado. Instituto Oceanográfico, Universidade de São Paulo, São Paulo.

Neste trabalho apresentamos dados de experimentos magnéticos e de fluorescência de raios X para o registro IODP U1471 localizado no Mar Interior das Maldivas. Além disso, apresentamos dados de experimentos magnéticos para o registro NAP63 localizado no embaiamento de São Paulo. Experimentos magnéticos forneceram uma visão da preservação da magnetita nos sedimentos do Mar Interior das Maldivas durante o início da diagênese. Aqui, apresentamos dados de remanência de alta resolução nos 15 metros superiores do registro sedimentar, e uma caracterização magnética detalhada em amostras discretas dos 5,5 metros superiores do registro IODP Site U1471. Pode-se demonstrar que a magnetita é rapidamente reduzida a greigita, com uma grande diminuição da magnetização remanente natural abaixo dos dois metros superiores do registro sedimentar. Os resultados sugerem que a diagênese atual poderia imprimir quase 100 mil anos de erro na cronologia baseada na magnetoestratigrafia. Dados de elementos obtidos no registro U1471 também forneceram uma visão detalhada das mudanças do sistema de monções indiano em escalas de tempo milenar. Com base em uma cronologia refinada ao longo dos últimos 550 mil anos, reconstruímos as mudanças no Sistema de Monções Indiano em uma escala de anomalias e verificamos suas relações com registros estabelecidos do Sistema de Monções do Leste Asiático. Com base nos registos de Fe/soma e Fe/Si, pode ser demonstrado que a aridez continental da Ásia acompanha as mudanças no nível do mar, enquanto a intensidade dos ventos das monções de inverno responde às mudanças na insolação de verão no hemisfério Norte. Além disso, as anomalias da aridez continental e a intensidade dos ventos das monções de inverno em eventos de escala milenar exibem poder na banda de precessão, quase em antifase com a insolação de verão no hemisfério Norte. A boa correspondência entre o nosso registo e os registos de anomalias das monções do Leste Asiático sugere a ocorrência de eventos áridos anómalos generalizados na Ásia. Neste mesmo registro, demonstramos ainda, com base na alta correlação da razão Fe/K com a suscetibilidade

magnética, que durante o Mioceno médio ao final, o local U1471 recebeu sua carga de sedimentos detríticos principalmente do Ganges-Brahmaputra. Nossos dados sugerem que durante o Mioceno médio e tardio, a elevação do Himalaia e do planalto tibetano fortaleceu as monções de verão indianas e aumentou a aridez no interior da Ásia, iniciando a deposição de argila vermelha no leste do planalto chinês de loess. No registro NAP63, coletado na Baía de São Paulo, demonstramos com base no registro do componente de alta coercividade da aquisição da Magnetização Remanente Isotérmica, que a entrada de sedimentos do Rio da Prata foi restrita devido aos fortes ventos de nordeste durante intensificação das monções de verão na América do Sul. Também demonstramos que durante eventos frios no hemisfério norte a monção de verão sul-americana foi intensificada.

Palavras-chave: Mioceno. Himalaia e platô Tibetano. Planalto chinês de loess. Eventos áridos generalizados na Asia. Eventos Heinrich.

CHAPTER 1. THE INDIAN SUMMER MONSOON

1 INTRODUCTION

1.1 THE MODERN INDIAN SUMMER MONSOON

During the Indian Summer Monsoon (ISM), rain falls preferentially on the western Indian coast under the topographic influence of the western Ghats, having a strong impact on lifestyle of millions of people, who are affected by extremely humid weather and depends on seasonal rainfall for agriculture. Today, the Indian subcontinent, is heavily affected by the seasonal windward inversion driven by the seasonal cycle of solar heating over the Northern Hemisphere related to the Indian monsoon system (IMS). While southwesterly winds dominate during the summer, bringing strong rainfall over the Indian-Asian land mass, in the winter, a high-pressure cell with anticyclonic circulation develops over central India blowing cold and dry northeasterly winds across the Indian east coast (Murty, 2021) (fig. 1) (Carrasqueira et al., 2023).

Actually, strong southwesterly winds dominate the annual mean atmospheric circulation in the northern Indian Ocean during boreal summer (Schiller and Godfrey, 2003), and together with northerly Shamal winds delivery a huge amount of aeolian dust sourced in Arabian Peninsula and Nubian desert into northwestern Arabian Sea (Ackerman and Cox, 1989; Yu et al., 2015) (fig. 1A).

Satellite data are useful to assess the flow of dust to the Maldives archipelago. Aerosol Optical Thickness and Aerosol Ångström Exponent are important parameters in understanding the status of ambient aerosol concentration. Aerosol Optical Thickness analyses are based on the fact that the particles change the way the atmosphere reflects and absorbs visible and infrared light. An Aerosol Optical Thickness of less than 0.1 indicates a crystal clear sky with maximum visibility, whereas a value of 1 indicates very hazy conditions (“Aerosol Optical Depth,” 2022). The Aerosol Ångström Exponent is basically a quantitative indicator and inversely proportional to the size of the aerosol particles. When the Aerosol Ångström Exponent is close to 1.0 is considered to be black carbon-rich aerosol from fossil fuel burning, and when it is higher than 1, it is often considered to be an indication of the presence of dust (Andreae and Gelencsér, 2006; Laskin et al., 2015; Moosmüller et al., 2009; Russell et al., 2010)

Satellite compiled data (2002-2020) from seasonal distribution of Aerosol Optical thickness, show an increase in the flux of aerosol in northwesterly Arabian Sea during Summer Monsoon ("L3 Browser - NASA Ocean Color," n.d.) (fig. 1B). Although the greatest flux of aeolian dust occurs in summer, only a small portion of this sediment reaches the eastern Arabian Sea where the Maldives Archipelago is located (Kunkelova et al., 2018; Lindhorst et al., 2019).

Summer monsoon winds also promote strong eastward surface ocean currents and limits the influence of low salinity surface waters from Bay of Bengal into eastern Arabian Sea (Stainbank et al., 2021). Moreover, due to increased precipitation during summer monsoon, higher input of organic matter at the northern Indian Ocean, promotes a southward expansion of the Arabian Sea oxygen minimum zone (Lachkar et al., 2018).

In the winter, northeasterly winds carry dust from deserts in Indian-Asian land mass to the eastern Arabian Sea. Satellite compiled data (2002-2020) from seasonal distribution of Aerosol Angstrom Exponent, show an increase in the flux of fine dust particles (high values) toward the Maldives Archipelago during winter monsoon (OceanColor, fig. 1E), clearly distinct from the input of coarse sediments (low values) during the summer ("L3 Browser - NASA Ocean Color," n.d.) (fig. 1D).

Changes in the lithogenic fraction of sediments from Maldives Inner Sea was previously associated with changes in the amount of aeolian dust transported from the Indian-Asian landmass during the winter monsoon (Bunzel et al., 2017; Kunkelova et al., 2018). This result was explained by the dominance of fine particles in the lithogenic fraction (Lindhorst et al., 2019).

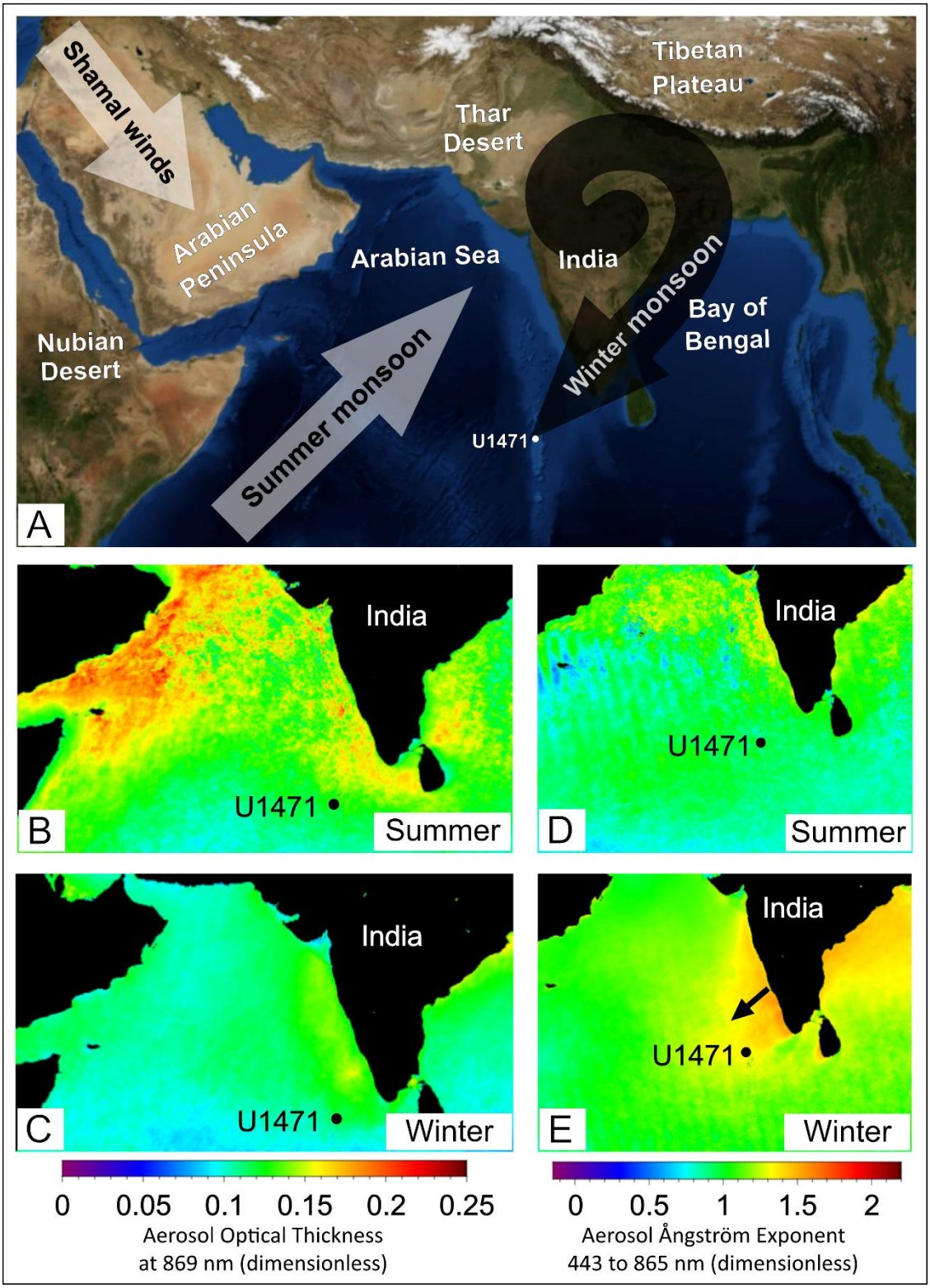

Figure 1. **Indian monsoon scheme.** (A) Satellite image of the IMS domain with the monsoon wind scheme during the summer (white arrows), and during the winter (black arrows). The figure also shows a satellite compiled data (2002-2020) from summer and winter distribution of the (B and C) Aerosol optical thickness at 869 nm and (D and E) Aerosol angstrom exponent 443 to 865 nm ("L3 Browser - NASA Ocean Color," n.d.). Black arrow indicates the direction of fine dust transport by northeasterly winds (Carrasqueira et al., 2023).

1.2 MALDIVES SETTING

The Maldives archipelago in the central equatorial Indian Ocean is an isolated tropical carbonate platform and constitutes most of the central part of the Chagos-Laccadives Ridge, which is in southwest India (fig. 2). The dual row of atolls oriented from north to south includes the Maldives inner sea. The atolls are separated from each other by channels between the atolls that go deeper toward the Indian Ocean (Purdy and Bertram, 1993). The Inner Sea is an internal basin with a water depth of up to 550 meters. The carbonate succession of the Maldives is almost 3 kilometers thick and has accumulated since the Eocene, far from any contribution of terrigenous sediments (Purdy and Bertram, 1993).

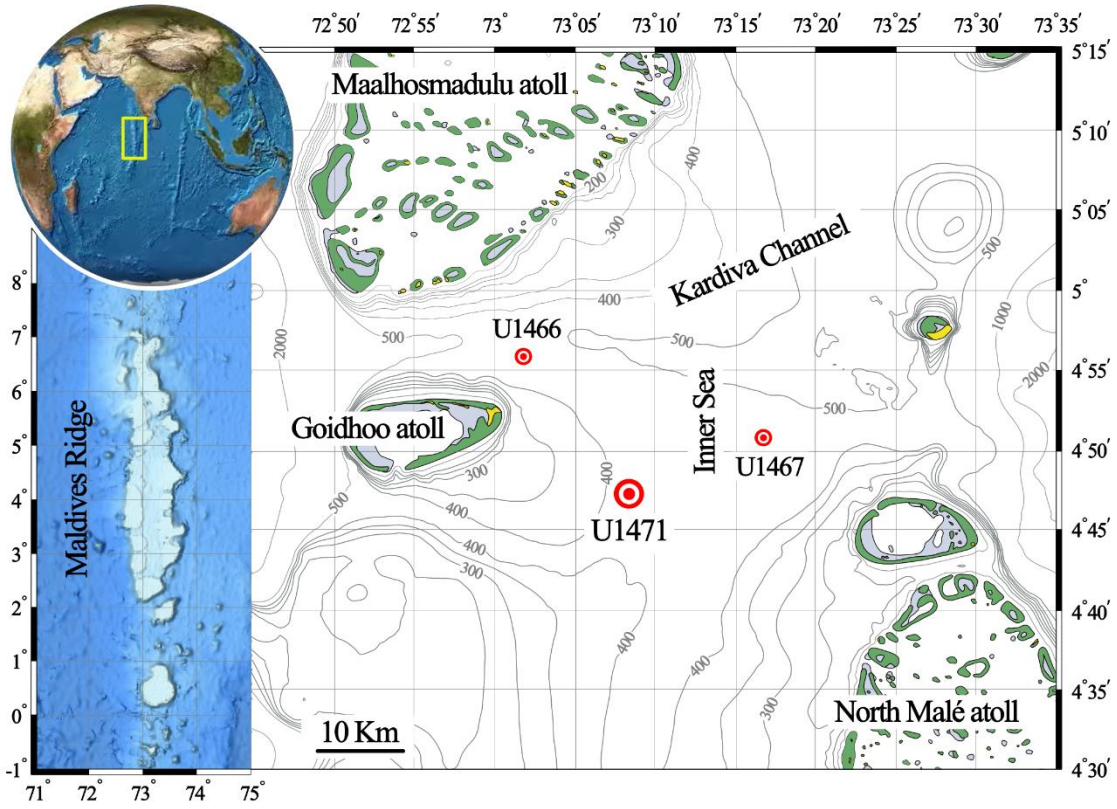

Figure 2. **Location of the site U1471.** Location of the Maldives Archipelago (yellow rectangle) along the central part of the Chagos-Laccadives Ridge in the Indian Ocean. The Site U1471 is situated in the deepest part of the Inner Sea near the outflow of the southern branch of the Kardiva Channel into the Inner Sea (adapted from Betzler et al., 2017a).

Carbonate production was established during the Eocene, when the carbonate banks flattened at the top began to form on topographical risings created by the volcanic

basement during the Eocene to the early Oligocene. By the end of the Oligocene, the banks had typically high edges separating the interior areas from the open ocean banks. During the lower and middle Miocene, including the mid-Miocene Climate Optimum, the growth of the bank occurred in silting and progressing pulses controlled by sea level fluctuations. The drastic change in the development of the carbonate building from a sea-level controlled system to a predominantly current-controlled system as revealed by seismic reflection data sets (fig. 3) which show that the carbonate building mainly contains sedimentary drift bodies, indicating that currents (e.g., environmental changes) were one of the main evolution factors (Betzler et al., 2013a, 2013b, 2009; Lüdmann et al., 2013). This drastic changes seems to be directly linked to the evolution of the Indian monsoon (Betzler et al., 2016).

It is proposed that upwelling from monsoon currents has shaped atolls in the past, controlling sediment production and reef growth. Thus, the partial drowning time of the shelf and the evolution of the monsoon are linked. In monsoon conditions, the upwelling injects nutrients into surface waters, affecting carbonate banks (Betzler et al., 2009). Even in the short term, seasonal upwelling forces the adaptation of carbonate organisms (Reijmer et al., 2012), which controls the biotic association with low growth potential and more vulnerability to the effects of sea level changes. This process caused the disappearance of the barrier reef, which was replaced by a chain-shaped reef, separated by passages that accommodate stream flow (Betzler et al., 2009; Lüdmann et al., 2013).

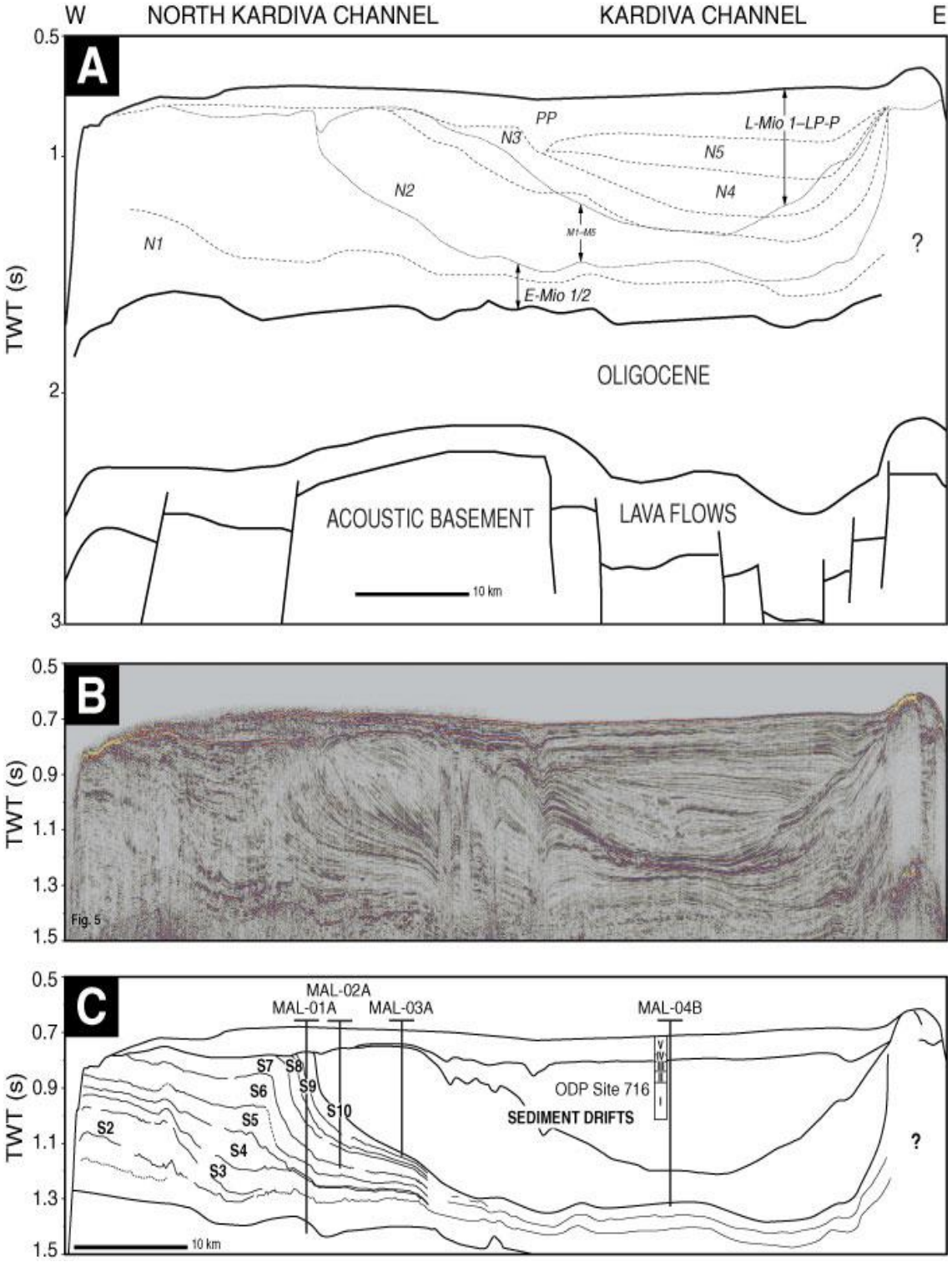

Figure 3. **The Maldives carbonate edifice.** (A) Seismic units in the Maldives carbonate building: N1-N5, PP (Aubert and Droxler, 1996) and E-Mio 1/2, M1-M5, L-Mio 1-LP-P according to (Belopolsky and Droxler, 2004). (B) NEOMA-P65 seismic line (vertical magnification = 20 ×) from west-east along South Maalhosmadulu and from the interatol channel Goidhoo. (C) General interpretation from high resolution seismic data for this study (Betzler et al., 2013a). I = Upper Miocene, II = Lower Pliocene, III = Medium Pliocene, IV = Upper Pliocene, V = Pleistocene.

The Maldivian archipelago margins toward the ocean usually have a steep slope, with dips of 20° to 30° until reaching a depth of 2000 m. On the Inner Seaside, atolls have the same diving angles, but reach water depths of about 150 meters, where the gradient decreases quickly (Fürstenau et al., 2010). The Inner Sea is characterized by the deposition of periplatform oozes (Droxler, 1990; Malone et al., n.d.), accumulated locally in drift sediments bodies (Betzler et al., 2009).

The sediments accumulating in the Maldives Inner Sea are mainly composed of pelagic test of foraminifers, pteropods, and coccolithophorids (mostly calcite and some aragonite) associated with fine bank-derived neritic carbonate particulates (mostly aragonite and some magnesian calcite), their variations through time reflect changes in equatorial Indian Ocean currents, upwelling, dust fertilization, and global sea level (Betzler et al., 2017a, 2013a, 2013b, 2009).

Sea-level is the fundamental driving force behind flooding and exposure of the shallow-water production areas, and thus fine bank-derived carbonate production and export. According to (Boardman et al., 1986; Droxler et al., 1983), during sea-level highstands, when carbonate platform flat tops are flooded, the Sr-rich aragonite production and export reach their maxima. This production falls during lowstands, when platform tops are exposed and karstified, restricting production to terraces.

In sediments from Maldives Inner Sea, (Paul et al., 2012), reported a very strong correlation between the aragonite record and the fine grain-size fraction. According to the authors, the sediment redistribution through ocean currents does not seem to influence the glacial-interglacial variations in aragonite and the fine grain-size fraction significantly. Furthermore, the author suggests that the aragonite content can be used to better quantify the timing and extent of changes in the Pleistocene Sea level.

1.3 SITE U1471

Site U1471 (fig. 2), drilled at 4°45'59''N and 73°08'07''E, in a water depth of 419.3 meters, is in the middle of the Maldives Inner Sea, on the most distal portion of a sediment drift attached to Goidhoo Atoll, one of the several western atoll chain. The Site offers the opportunity to access the aridity history in the Indian-Asian land mass and the Arabian Peninsula recorded in upper Cenozoic periplatform extended drift sediment sequence. Variations through time of bank-derived fine aragonite coupled with pelagic

oxygen isotope records have demonstrated, based on the analyses of the Plio-Quaternary periplatform sequence recovered in Ocean Drilling Program (ODP) Site 716, the great paleoclimatic potential of these periplatform sediment accumulations (Droxler, 1990).

According to the preliminary reports produced aboard the Joydes Resolution ship, a succession of 889 m of drift deposit was recovered at Site U1471. Seven lithostratigraphic units are distinguished in drift deposits that reflect the degree of progression controlled by current and diagenic overprinting (fig. 4) (Betzler et al., 2017a, p. 147).

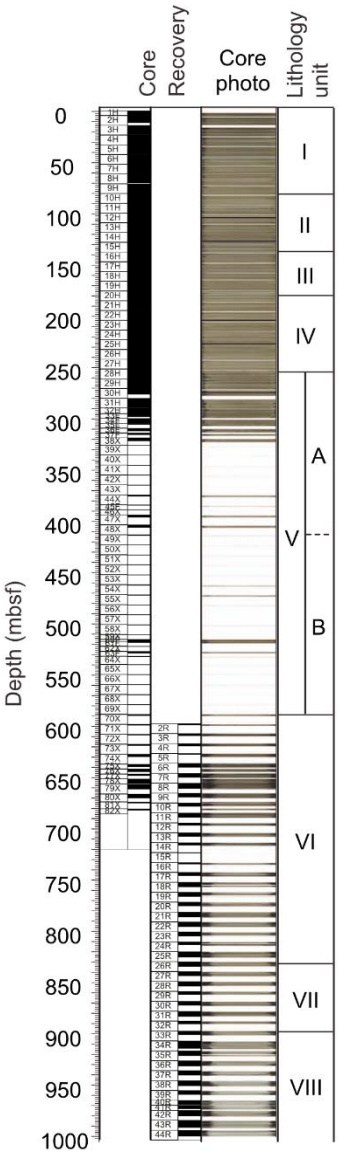

Unit I: unlithified planktonic foraminifer–rich packstone to wackestone.

Unit II: unlithified to partially lithified foraminifer-rich packstone.

Unit III: unlithified to partially lithified planktonic foraminifer– rich wackestone.

Unit IV: unlithified to lithified planktonic foraminifer–rich packstone.

Unit V: dominantly lithified planktonic foraminifer–rich packstone.

Unit VI: alternations of planktonic foraminifer–rich packstone and wackestone.

Unit VII: alternations of planktonic foraminifer–rich and bioclastic- rich grainstone.

Unit VIII: alternations of foraminifer-rich packstone to wackestone and wackestone to mudstone.

Figure 4. **U1471 core log.** Core recovery from ~1003 m thick succession of site U1471, core photograph and the units identified through lithology (Betzler et al., 2017a, p. 147).

Biostratigraphic and paleoenvironmental analyses conducted at holes U1471A, U1471C and U1471E provided a first age model for the Site U1471 (fig. 5) (Betzler et al., 2017a, p. 147). Interval A contains a succession of well-constrained events that indicate an average sedimentation rate of 4.0 cm/kyr. In the Pliocene–Pleistocene interval, however, a consistent offset occurs between ages inferred from calcareous nannofossil events and those inferred from planktonic foraminifers, with the planktonic foraminifers suggesting ages about 0.5 million years (Myr) older than the calcareous nannofossils. This pattern was also observed in the Pliocene–Pleistocene sequence of Sites U1465 and U1467, which points to a possible problem with the age calibrations of these events for this region. In Interval B, sufficient planktonic foraminiferal and nannofossil events were recognized, and their ages reasonably agree with each other. The inferred average sedimentation rate for this interval is 8.0 cm/kyr (Betzler et al., 2017a, p. 147).

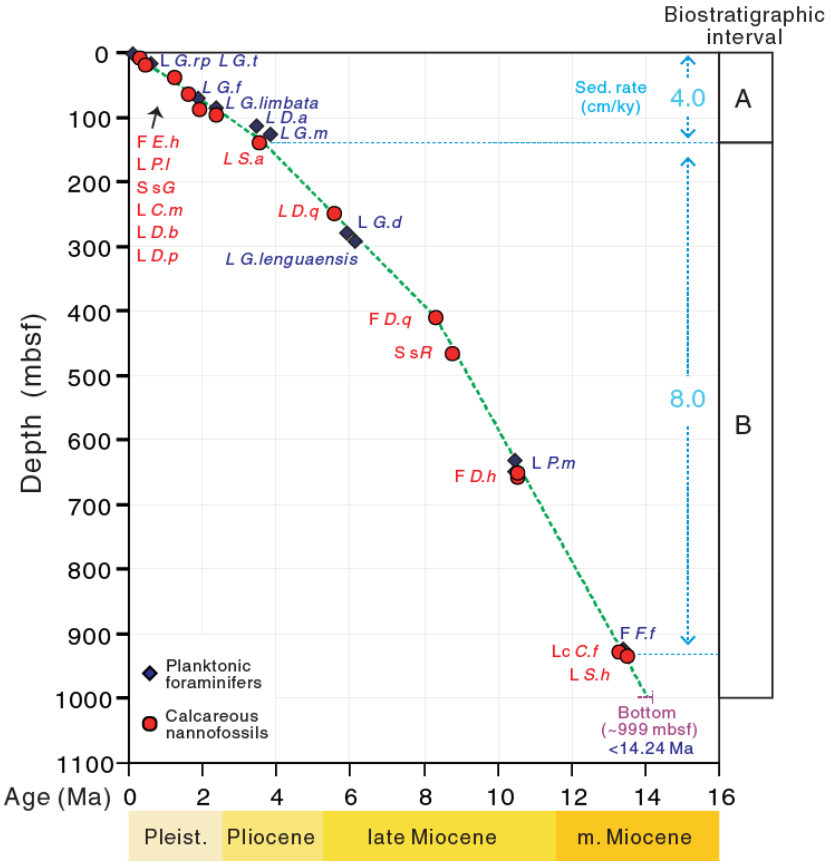

Figure 5. **Bioevents from site U1471.** Age model obtained based on biostratigraphic events and paleoenvironmental analyses combining Holes U1471A, U1471C, and U1471E (Betzler et al., 2017a, p. 147).

The Natural Remnant Magnetization (NRM) data from the U1471 record obtained on board the ship (Betzler et al., 2017a) show a peak in intensity at depth of 700 to 600 meters below sea floor (mbsf), up to a thousand times greater than the current values (fig. 6), making it a range of interest for the paleomonsoon study.

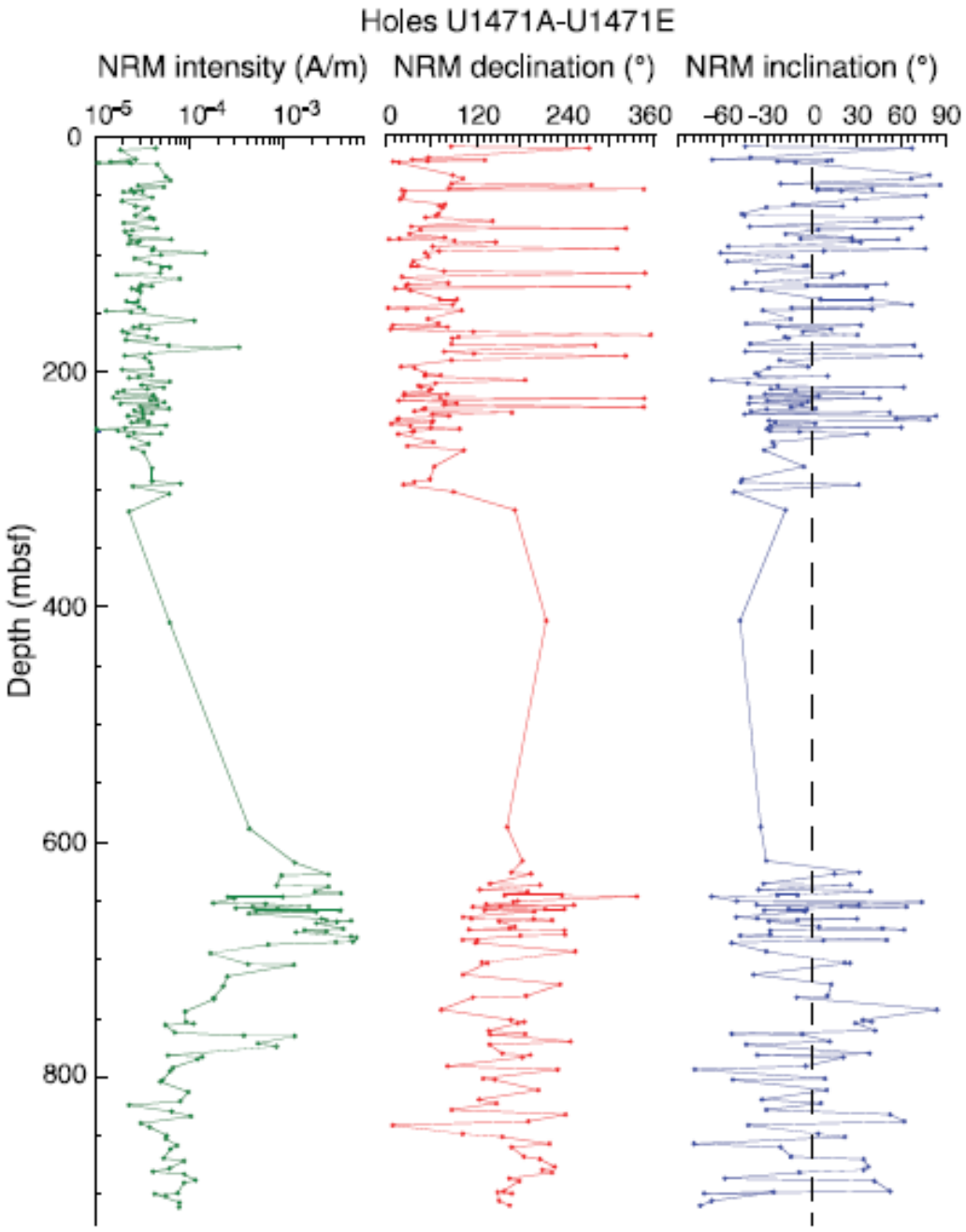

Figure 6. **NRM of site U1471 between zero and 840 mbsf**. From left to right, NRM intensity, declination, and inclination from discrete samples without demagnetization, Holes U1471A and U1471E (Betzler et al., 2017a, p. 147).

1.4 OBJECTIVES

This work aims to reconstruct the ISM for some periods of Neogene, through recognizing changes in the coupled atmospheric and oceanographic processes that control the carbonate production and transport of terrigenous sediments to the Maldives inner sea, in response to the main climatic events occurred by that time.

The objective was made possible through an integrated study of the magnetic properties compared to the composition of elemental ratios obtained in the U1471 record drilled by International Ocean Discovery Program's (IODP) expedition 359 in Maldives Inner Sea.

1.4.1 Specific Goals

Some challenges in reconstruct the continental rainfall in the ISM domain lie in obtaining an accurate chronology and an in-depth understanding of how the different environmental processes controls the investigated properties in our record.

To obtain an accurate chronology, some of previous works on ISM caried in sedimentary records from Maldives Inner Sea constructed their age models based on the magnetostratigraphy (e.g., Betzler et al., 2017a; Lanci et al., 2019). In marine sedimentary records, magnetite is the main magnetic carrier of the paleogeomagnetic field, and its preservation is crucial to the chronology reliability. To date, there is no detailed study about the magnetite preservation in Maldives Inner Sea sediments during early diagenesis. In this topic, this work aims to:

(1) Carry out a detailed study of the magnetic properties in the first meters of the record to deepen knowledge about local diagenetic processes that could affect the preservation of the geomagnetic record.

(2) Accurate the chronology using geomagnetic data.

The sedimentary records drilled in the Maldives Inner Sea suggests that, in the last 500 kyr, the wind intensity and arid conditions in the dust source areas are related mainly to precession and eccentricity cycles (Kunkelova et al., 2018; Lindhorst et al., 2019). These studies show the enormous potential of the Maldives dust record in the ISM research. However, prior to the present work (Carrasqueira et al., 2023), there was no publication on IMS anomalies from records in the Maldives. The occurrence of

anomalous arid conditions was observed in a 640 kyr-long stalagmite $\delta^{18}O$ record from Sanbao cave situated in central China (Cheng et al., 2016). This work aims to:

(3) Reconstruct the mid-late Pleistocene ISM in high resolution and relate it to the orbital forcing.

(4) Remove the orbital signal from the data to assess ISM anomalies.

Determining the causes to the ISM onset has been a subject of great efforts, but there is still no consensus on when this happened. Previous studies reported the ISM onset to occur at 8.5 Million years ago (Ma) (Kroon et al., 1991; Prell and Kutzbach, 1992; Zhisheng et al., 2001), at 11 Ma (Rea, 1992; Zheng, 2004), and more recently at 12.9 Ma (Betzler et al., 2016). In addition, there is also no consensus on the main mechanisms that would have triggered the ISM onset. Was suggested that the Himalayan uplift boosted the Asian monsoon (Clift et al., 2008; Rea, 1992; Zheng, 2004). In contrast, (Betzler et al., 2016) argued that the ISM onset, occurred too fast to be solely explained by tectonic processes. These different results, denotes a poorly knowledge about the climatic control on the records. This work aims to:

(5) Relate our record to previously published works about ISM and the main climatic events occurred by that time to expand knowledge about the response of Maldives Inner Sea record to environmental processes.

(6) Reconstruct the ISM rainfall between 12.5 and 9.5 Ma using elemental and magnetic data.

1.4.2 Hypothesis

The lithogenic fraction of sediments from Maldives Inner Sea is widely interpreted as wind blow dust, increased during dry periods. To reconstruct the ISM evolution, previous works interpreted the iron content and the magnetic susceptibility as changes in aridity extension in Indian subcontinent (Betzler et al., 2017a; Kunkelova et al., 2018; Lanci et al., 2019). The present work will test the followed hypothesis.

(1) Maldives Inner Sea receives its load of lithological sediments mainly by the aeolian dust blow.

(2) Changes in continental aridity controls the supply of lithological sediments to the Maldives Inner Sea.

(3) Magnetic susceptibility increased in response to expansion of the arid zones.

(4) The long-term continental rainfall at ISM domain was affected by tectonic events related to Himalaya and Tibetan Plateau uplift.

(5) After the mid-late Pleistocene, ISM was controlled mainly by NHSI.

CHAPTER 2. THE SOUTH AMERICA SUMMER MONSOON

2 INTRODUCTION

2.1 SUMMARY OF LAST 40 KYR PALEOCLIMATE

2.1.1 The Last glacial termination

Quaternary glacial-interglacial cycles spanned roughly 100 kyr, during which the ice sheets slowly expanded over 80–90 kyr, whereas glaciation usually ended within 10 kyr. The last glacial termination, between about 20 to 8 kyr ago, underwent several abrupt climatic and marine oscillations that punctuated a period of generally rising temperature and sea level.

At the end of the Last Glacial Maximum (LGM), NHSI started increasing at ~21 ka reaching a peak at ~11 Ka. Between 20 and 15 kyr, atmospheric levels of CO_2 increased, and Antarctic temperatures climbed while sea level slowly ascended from its low stand during the LGM of about 120 m below present (Gornitz, 2021). Sea level rise accelerated during the mild Bölling/Allerød Interstadial at ~14.6 to 13 kyr, at a time of decreased Antarctic temperatures. The Bölling/Allerød warming ended with an abrupt transition to a 1 kyr cold phase, the Younger Dryas interval (12.8–11.7 kyr), while Antarctic temperatures warmed (Gornitz, 2021). The rapid termination of the Younger Dryas cooling occurred within just a few decades (Steffensen et al., 2008). This climatic reversal effectively ended the last glaciation and ushered in the Holocene Epoch. A bipolar-seesaw mechanism may have been responsible for the late phases of hemispheric asymmetric climate, similar to the climatic pattern described for Heinrich events (Gornitz, 2021).

2.1.2 Heinrich events

Heinrich events are defined as cold periods in the Northern Hemisphere, lasting an average of 500 years. It is characterized by layers of ice rafted debris (IRD) dropped into the North Atlantic from melting icebergs (Hemming, 2004). IRDs were deposited

when Greenland temperatures had dropped 3–5 °C. Heinrich events occurred on an average of every 5 to 6 kyr. One hypothesis holds that as a growing ice sheet reaches a critical mass, it becomes increasingly unstable (Gornitz, 2021). The accumulated weight of the ice causes the basal ice sheet to melt by pressure, separating large chunks of ice from the glacier and allowing it to advance on a lubricated base.

The cold phase of Heinrich events occurred at a time of warming in the Southern Hemisphere. The bipolar-seesaw hypothesis proposes episodic reversals in deep ocean circulation (Gornitz, 2021). Massive iceberg influxes or freshwater outbursts from subglacial lakes reduce northern Ocean salinity, slow down the Gulf Stream-North Atlantic current, and weaken North Atlantic Deepwater formation. A diminished thermohaline circulation drives heat build-up farther South, enhancing ice growth. Once Northern Hemisphere temperatures recover and North Atlantic Deepwater formation resumes, ocean heat transport moves northward while the Southern Hemisphere cools.

During the last 40 Kyr, four Heinrich events have been identified. The event H4 occurred at 38 Ka, event H3 occurred at 32.7-31 Ka, event H2 occurred at 26.5-24 Ka and event H1 occurred at 16.9-15.4 Ka (Harrison and Sanchez Goñi, 2010; Hemming, 2004; Weldeab et al., 2006).

2.2 THE MODERN SOUTH AMERICA SUMMER MONSOON

The South American Monsoon System is part of the monsoon system of the Americas and develops over a large extension of the South American continent in a region that compasses from the Amazon Forest crossed by the Equator to the La Plata Basin, passing through the high and sharp Andes mountains that rise along the Pacific coast on the west and across the driest desert (Atacama), as well as a high desert in the Brazilian highlands.

The seasonal pattern of rainfall over South America is mainly related to land–sea thermal contrast that causes changes in low- and high-level atmospheric circulation (Vera et al., 2002; Zhou and Lau, 1998). During the austral summer, South American rainfall develop as a result of intense convection over the interior of the Amazon basin (Zhou and Lau, 1998). The equatorial winds that carry moisture westward from the tropical Atlantic through the Amazon basin to the Andes, are blocked by the high

mountains and forced to the southeast by a northwesterly low-level flow know as South American low-level jets that transports the moisture from Amazon basin to the centre and southeastern Brazil (Gan et al., 2004) (fig. 42). This moisture carried by low-level jets forms a band with instability clouds called the South Atlantic Convergence Zone (SACZ; fig. 42). The SACZ reaches maximum intensity in austral summer in phase with Amazon basin convection (Cruz et al., 2005), and despite it is far from their centre of convective activity, summer rainfall in southeastern Brazil is strongly influenced by the southward progression of convection across the Amazon basin (Cruz et al., 2005). In Southeastern Brazil, rainfall is composed of a mixture between the source of Amazon basin and the nearby Atlantic source (fig. 42). The SACZ region is of particularly importance due to the hydroelectricity generation and the agricultural base of local economies. The moisture flux across the Amazon Forest is important for maintenance of the SACZ, it is believed that the deforestation of the Amazonian intertropical forest can cause dry conditions in southeastern Brazil (Nobre et al., 2016).

During the austral winter and early spring, equatorward incursions of southern fronts (fig. 42) result in cyclonic storms that carry moisture inland from the nearby Atlantic Ocean (Vera et al., 2002). The southern westerly wind belt has also played an important role in the climatic conditions over S and SE South America blowing moisture from the Pacific at the tropospheric level to the Andes (Razik et al., 2013) and bringing dust from the west to the Atlantic Ocean (Gaiero et al., 2003; Garreaud et al., 2009). During glacial periods the dry climate contributed to a deeper erosion of the Andean Cordillera and propelled the formation of the Pampean loess deposits (Gaiero et al., 2007, 2003; Iriondo et al., 2009; Maher et al., 2010; Prospero et al., 2002; Terminiello et al., 2001; Zárate and Blasi, 1993).

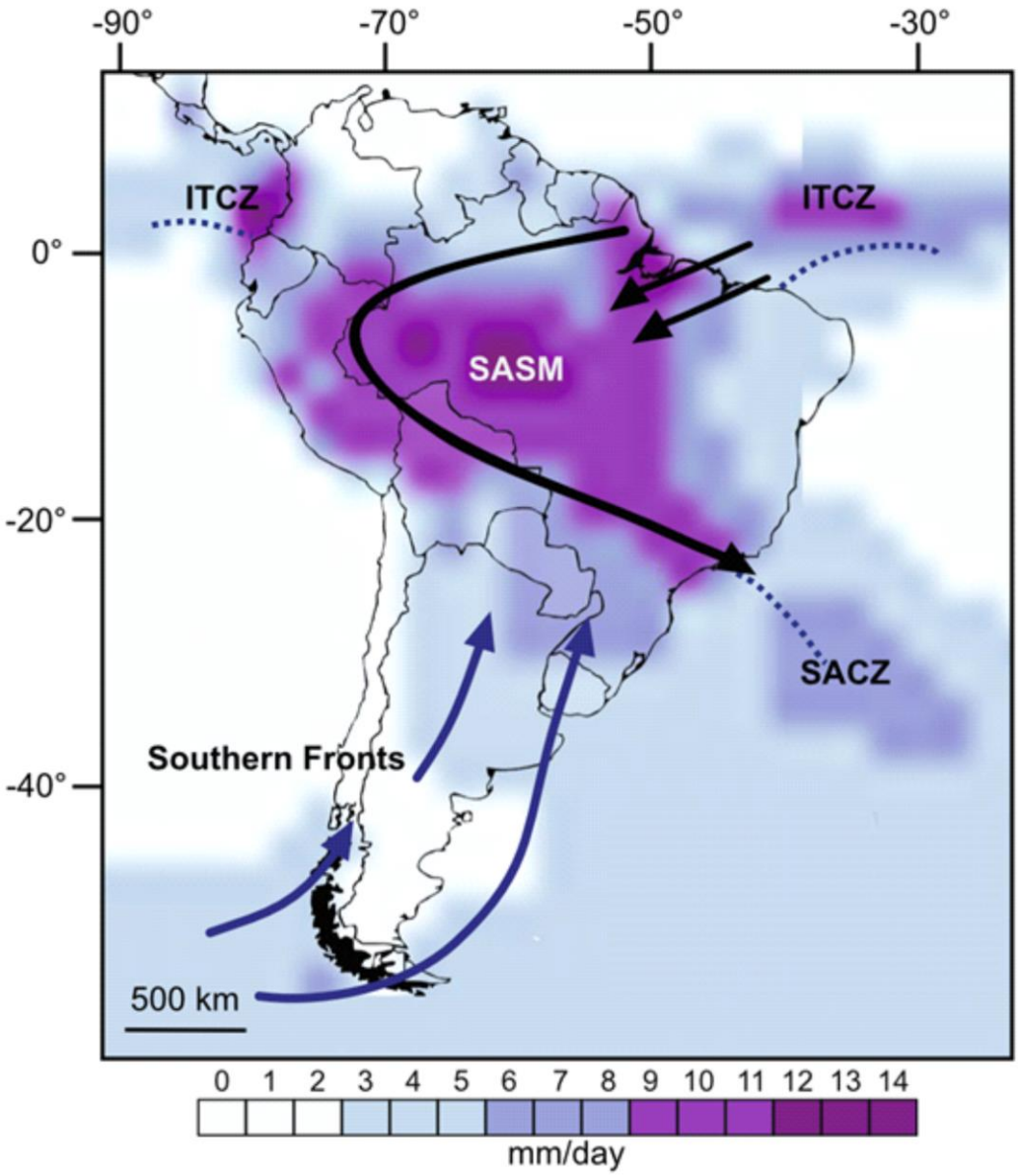

Figure 7. **South America monsoon scheme.** Map of South America, showing the long-term mean annual precipitation from 1981 to 2010 using the data from the Global Precipitation Climatology Project (Adler et al., 2003). The SASM (black arrows), and the position of the ITCZ and SACZ (blue dashed lines) during the austral summer in South America (DJF). Blue arrows show the northernmost position of the year-round southern fronts (adapted from Rodríguez-Zorro et al., 2020).

2.2.1 The insolation drives the SASM

Periods of high SHSI resulted in increased convection over Amazon interior and in maximum movement of the SASM/SACZ to the south (Cruz et al., 2005). In addition to the movement of the monsoon a general intensification of the mean zonal Hadley circulation and tropical convective activity may have accompanied these shifts. This

mechanism is also valid for the short-term trend during the Younger Dryas period, which is consistent with rapid southward movement of the South American monsoon (Cruz et al., 2005). During SHSI minima, the mean location of the SASM and the SACZ shift northward, and less moisture from Amazon basin is transported towards the southeast, decreasing the relative contribution of summer monsoonal rainfall to the southeast Brazil (Cruz et al., 2005).

2.3 SÃO PAULO BIGHT SETTING

The São Paulo Bight is the arc-shaped part of the eastern Brazilian margin extending from 23°S to 28°S (Zembruscki, 1979). Its bottom shows a complex morphology involving channels, canyons, and considerable variations in slope morphology (Furtado et al., 1996). The shelf break is in a water depth of approximately 140 meters, with the upper slope showing an average gradient of approximately 1:55. The slope is generally smooth and has a slightly concave profile, characteristic of depositional margins (Zembruscki, 1979).

Due to the absence of significant discharges of rivers, the sedimentation in the Brazilian southeastern margin is strongly dominated by a dynamic of oceanic water masses and circulation on the platform, these processes control the primary production and sediment redistribution in the area, moreover in the south of São Sebastião, the depositional processes are associated with seasonal influence of the plume of River de la Plata (Mahiques et al., 2004) carried by the coastal water in the internal platform.

The hydrodynamic conditions in the internal platform are strongly dominated by the wind, where the waves generated direct the currents (Mahiques et al., 2002). In the middle and outer shelves as well as in the upper slope sedimentary processes seem to be influenced by the Brazil Current (BC) flow along the south-western Atlantic continental margin (Campos et al., 1995, 2000; Müller et al., 1998; Stramma and England, 1999). Nearby of São Sebastião Island the dominant offshore flow of BC meandering added to the offshore flow of coastal water intensifies the transport of suspended sediments into the regions of outer shelf and upper slope (Mahiques et al., 1999; 2002).

The sediments between the inner and outer platform exhibit characteristics which vary from the siliciclastic to carbonate, respectively, while the slope is characterized by the

deposition of hemipelagic sediments and turbidites (Mahiques et al., 2002).

2.3.1 Sediment delivery to São Paulo Bight

The main sediment sources that contribute for the terrigenous fraction in São Paulo Bight are the suspended material carried with RdlP plume and the aeolian dust originated in Andean Mountains.

The sediments delivered with RdlP plume strong depends on the coastal circulation. The seasonal variability of the RdlP plume in the last decades is mainly identified by salinity fluctuations along the coast, with a northward penetration to 28°S during austral winter and a retraction to 32°S during austral summer (Piola et al., 2008, 2005, 2000), meantime, different lines of evidence suggest that the weathering products of the Paraná basalts delivered to the ocean by the RdlP can reach the SE Brazilian continental shelf as far north as 25°S (Mahiques et al., 2008). It is important to point out that during El Niño years despite the higher runoff of RdlP, the influence of RdlP plume retracts to the south due to the strengthening of northeast winds (Piola et al., 2008).

The rainfall over the RdlP drainage basin is directly affected by the SASM (Chiessi et al., 2009; Cruz et al., 2005). The RdlP drainage basin comprises a catchment area which encompasses a large surface of the Paraná flood basalts and the subordinated acidic volcanics. Basalts from Paraná Magmatic Province have a magnetic mineralogy mainly dominated by magnetite and titanomagnetite, both fine (SD) and coarse (MD) and their oxidation products, such as maghemite and hematite (Tamrat and Ernesto, 1999). Most of the suspended material transported into the RdlP derives from the erosion of Paraná volcanics (e.g., Depetris et al., 2003; Garming et al., 2007; Laprida et al., 2007).

A second main source of sediments to the SE Brazilian shelf is the Andean dust transported eastward by the westerlies (Gaiero et al., 2003) and deposited on the Argentinean Pampas in an extensive loess sequence (Maher et al., 2010). These sediments comprise the main source of fine-grained particles that reach the Southwestern Atlantic and the Southeastern America. The dust from southern South America, is characterized by the presence of fine-grained magnetite (Orgeira et al., 2008) and detrital (titano-)magnetite (Orgeira et al., 2009; OrgeIra et al., 1998).

Changes in magnetic mineralogic related to changes in sediment delivery to the São Paulo Bight from low coercive phases (e.g., magnetite) present in the Pampean loess (Orgeira et al., 2009) to high coercive phases (e.g., hematite) that originated from the flood basalts of the Paraná Basin (de Oliveira et al., 2002) allow to reconstruct the SASM.

2.4 SITE NAP 63

The site NAP63 was located at 24°50'26''S, 44°19'00''W to a depth of 840 meters (fig. 43). The site is in the area of the Intermediate Western Boundary Current (IWBC), which is located between 800 and 1100m water depth (Schmid et al., 2000). The IWBC flow northward, in opposition to BC, as well as the Deep Western Boundary Current, both flowing southwards. The region has muddy bottom, ideal for the study of high-resolution records. The NAP63 record was acquired with a gravity corer providing a continuous record of 2.25 m length.

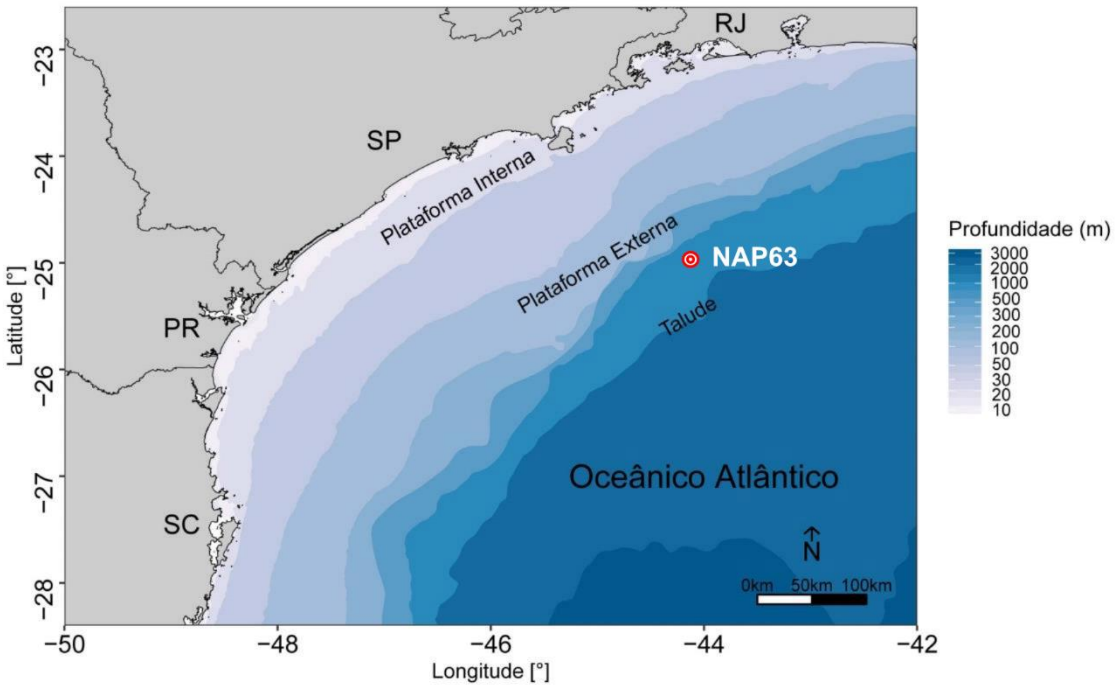

Figure 8.. **Location of the site NAP63.** Map of São Paulo Bight with the NAP 63 site identified on the middle slope. The gradient in blue color indicates the bathymetric variation from the lightest, from 0-20 m deep, to the darkest, up to 4000 m deep.

2.5 OBJECTIVES

This work aims to reconstruct the South American Summer Monsoon (SASM) for the last 40 Kyr on the scale of millennial events. The objective was made possible

through the magnetic studies of changes in the relative concentrations of low and high coercivity minerals obtained from the NAP63 record drilled on the slope of São Paulo Bight.

The supply of detrital material to the São Paulo Bight is mainly composed of magnetite-rich aeolian dust (low coercivity) originated by the erosion of the Andes and by a hematite-rich fluvial fraction (high coercivity) from the Paraná basin which flows into the Rio de la Plata (RdlP) (de Oliveira et al., 2002; Mathias et al., 2014; Orgeira et al., 2009).

2.5.1 Specific Goals

Most of the records used for the SASM study were obtained from speleothems (e.g., Cruz et al., 2005), they suggest that precipitation tracks the Southern Hemisphere summer insolation (SHSI) in phase with the February insolation at 30°S. In this topic, this work aims to provide a marine record on SASM in which we can:

(1) Identify the orbital component of SASM and determine its phase relationship with the astronomical solutions.
(2) Recognize millennial-scale events such as Heinrich Stadials.

2.5.2 Hypothesis

The magnetic mineralogic obtained from a core drilled in São Paulo Bight mid-shelf (Mathias et al., 2014) describe changes in sediment delivery to the SE Brazilian shelf from fine-grained low coercive phases (e.g., magnetite) present in the Pampean loess (Orgeira et al., 2009) to coarse-grained low coercive phases plus high coercive phases (e.g., hematite) that originated from the flood basalts of the Paraná Basin (de Oliveira et al., 2002). The present work will test the followed hypothesis.

(1) The content of high coercivity minerals (e.g., hematite) increased during high SHSI.
(2) Millennial-scale events such as Heinrich Stadials, characterized by cold anomalies in the Northern Hemisphere, presented an opposite response in the Southern Hemisphere, in the form of strong SASM.

3 CONCLUSIONS

In this work we discussed the records IODP U1471 located in the Maldives Inner Sea and NAP63 in the São Paulo Bight, deepening de knowledge about the ISM and SASM, and in how the different environmental processes control the investigated properties in our records.

In the upper 5.5 mbsf of record U1471, we studied in detail the changes in magnetic characteristics and demonstrate that local diagenetic processes affect the preservation of the geomagnetic record. We demonstrate that currently, the reduction of magnetite and the subsequent authigenic formation of greigite in the upper meters of the record destroyed the ChRM, imprinting a secondary NRM with a delay of ~100 kyr.

We reconstructed the mid-late Pleistocene ISM in high resolution and relate it with the main climatic forcings. We show that during the last 550 kyr the IWMW responds directly to changes in NHSI, while the ISM rainfall tracks sea-level changes, and therefore incorporates the delay associated with changes in global ice volume. We also show that although ISM rainfall is primarily driven by global ice volume, arid conditions persisted in the Indian-Asian landmass during sea level rise in the MIS 8/7 transition, a period that was also characterized by WEAMI. The occurrence of extended aridity in our record concomitant with WEAMI indicates that the T-III was characterized by anomalous widespread arid conditions in Asia. We accessed the anomalies in the ISM by removing the effect of NHSI on the IWMW record and the effect of global ice volume from the continental arid record. Records showed that anomalous arid events on the Indian-Asian landmass and stronger IWMW were driven by increasing NHSI. Our results indicate that the ISM anomaly is dampening the direct effect of insolation, which could have led to greater control of changes in ice volume at high latitudes over the monsoon system at low latitudes.

During the mid to late Miocene, contrary to what has been widely held, we show that the detrital sediment delivered to Maldives Inner Sea was mainly represented by sediments from the Ganges-Brahmaputra. We identified that from 12.3 to 11.2 Ma the ISM rainfall strengthened in opposition to the general trend of global cooling/atmospheric pCO_2, possibly in response to the HTP uplift, leading to an intensification of aridity in the interior of Asia, which would have triggered the onset of

red clay formation in the eastern CLP. We also show that after 11.2 Ma the ISM rainfall weakened, possibly in response to the onset of upwelling in Oman margin, which would have led to the cooling of the SST in the northwestern Arabian Sea impacting the moisture advection in the region. Furthermore, we show that productivity in Maldives carbonate factory remained low up to 10 Ma, forced by the low nutrient content in the Indian Ocean surface waters during the carbonate crash.

In record NAP63, we show that, contrary to what was expected, the content of high coercivity minerals (e.g., hematite) decreased during high SHSI. We identified that the influence of the RdlP plume retracted to the south, due to strong northeasterly winds during periods of SASM intensification. Furthermore, we show that the SASM intensified during the Heinrich events, suggesting that ice growth in the Northern Hemisphere would have increased the thermal gradient between the hemispheres and forced the ITCZ southward.

The Indian and South American summer monsoons both develop due to the thermal gradient generated between the ocean and the continent, which causes strong moisture convection. These two monsoon systems, although forced by their characteristic boundary conditions, which make each of these systems unique, they are also driven by some global forcings such as atmospheric pCO_2, global ice volume and insolation. The Indian and South American monsoons may have different phase relationships between them depending on the type of forcing. For changes in atmospheric pCO_2 and global ice volume, an in-phase response is expected between the two climate systems. However, the lack of records covering SASM in at least some glacial cycles remains the biggest challenge to confirm this relationship. For changes in insolation or ice volume distribution between the two hemispheres, the Indian and South American monsoons present an anti-phase relationship with each other. The different responses of these two monsoon systems to different climatic forcings can be used to determine the nature of the forcing that has been acting, and thus, the study of these different monsoon systems in an integrated way of a global monsoon would provide a great advance in knowledge. Furthermore, the Indian and South American monsoons are such intense weather systems and cover such a huge area that they can change the global climate and thus must be considered as a driver of climate change.

References

Abdulkarim, M.A., Muxworthy, A.R., Fraser, A., Neumaier, M., Hu, P., Cowan, A., 2022. Siderite occurrence in petroleum systems and its potential as a hydrocarbon-migration proxy: A case study of the Catcher Area Development and the Bittern area, UK North Sea. J. Pet. Sci. Eng. 212, 110248. https://doi.org/10.1016/j.petrol.2022.110248

Ackerman, S.A., Cox, S.K., 1989. Surface weather observations of atmospheric dust over the southwest summer monsoon region. Meteorol. Atmospheric Phys. 41, 19–34. https://doi.org/10.1007/BF01032587

Adler, R.F., Huffman, G.J., Chang, A., Ferraro, R., Xie, P.-P., Janowiak, J., Rudolf, B., Schneider, U., Curtis, S., Bolvin, D., Gruber, A., Susskind, J., Arkin, P., Nelkin, E., 2003. The Version-2 Global Precipitation Climatology Project (GPCP) Monthly Precipitation Analysis (1979 Present). J. Hydrometeorol. 4, 1147. https://doi.org/10.1175/1525-7541(2003)004<1147:TVGPCP>2.0.CO;2

Aerosol Optical Depth [WWW Document], 2022. URL https://earthobservatory.nasa.gov/global-maps/MODAL2_M_AER_OD (accessed 9.26.22).

Alonso-Garcia, M., Rodrigues, T., Abrantes, F., Padilha, M., Alvarez-Zarikian, C.A., Kunkelova, T., Wright, J.D., Betzler, C., 2019. Sea-surface temperature, productivity and hydrological changes in the Northern Indian Ocean (Maldives) during the interval ~575-175 ka (MIS 14 to 7). Palaeogeogr. Palaeoclimatol. Palaeoecol. 536, 109376. https://doi.org/10.1016/j.palaeo.2019.109376

Andreae, M.O., Gelencsér, A., 2006. Black carbon or brown carbon? The nature of light-absorbing carbonaceous aerosols. Atmospheric Chem. Phys. 6, 3131–3148. https://doi.org/10.5194/acp-6-3131-2006

Aubert, O., Droxler, AndréW., 1996. Seismic stratigraphy and depositional signatures of the Maldive carbonate system (Indian Ocean). Mar. Pet. Geol. 13, 503–536. https://doi.org/10.1016/0264-8172(96)00008-6

Belopolsky, A.V., Droxler, A.W., 2004. Seismic Expressions and Interpretation of Carbonate Sequences: The Maldives Platform, Equatorial Indian Ocean. https://doi.org/10.1306/St49974

Berner, R.A., 1984. Sedimentary pyrite formation: An update. Geochim. Cosmochim. Acta 48, 605–615. https://doi.org/10.1016/0016-7037(84)90089-9

Betzler, C., Eberli, G., Kroon, D., Wright, J., Swart, P., Bejugam, N., Zarikian, C., Alonso Garcia, M., Bialik, O., Blättler, C., Guo, J., Haffen, S., Horozal, S., Inoue, M., Jovane, L., Lanci, L., Laya, J.C., Ling, A., Lüdmann, T., Young, J., 2016. The abrupt onset of the modern South Asian Monsoon winds. Sci. Rep. 6. https://doi.org/10.1038/srep29838

Betzler, C., Eberli, G., Zarikian, C., Alonso Garcia, M., Bialik, O., Blättler, C., Guo, J.A., Haffen, S., Horozal, S., Inoue, M., Jovane, L., Kroon, D., Lanci, L., Laya, J.C., Ling, A., Lüdmann, T., Nakakuni, M., Bejugam, N., Niino, K., Z., Y., 2017a. Site U1471. https://doi.org/10.14379/iodp.proc.359.109.2017

Betzler, C., Eberli, G., Zarikian, C., Alonso Garcia, M., Bialik, O., Blättler, C., Guo, J.A., Haffen, S., Horozal, S., Inoue, M., Jovane, L., Kroon, D., Lanci, L., Laya, J.C., Ling, A., Lüdmann, T., Nakakuni, M., Bejugam, N., Niino, K., Z., Y., 2017b. Site U1467. https://doi.org/10.14379/iodp.proc.359.105.2017

Betzler, C., Eberli, G.P., Lüdmann, T., Reolid, J., Kroon, D., Reijmer, J.J.G., Swart, P.K., Wright, J., Young, J.R., Alvarez-Zarikian, C., Alonso-García, M., Bialik, O.M., Blättler, C.L., Guo, J.A.,

Haffen, S., Horozal, S., Inoue, M., Jovane, L., Lanci, L., Laya, J.C., Hui Mee, A.L., Nakakuni, M., Nath, B.N., Niino, K., Petruny, L.M., Pratiwi, S.D., Slagle, A.L., Sloss, C.R., Su, X., Yao, Z., 2018. Refinement of Miocene sea level and monsoon events from the sedimentary archive of the Maldives (Indian Ocean). Prog. Earth Planet. Sci. 5, 5. https://doi.org/10.1186/s40645-018-0165-x

Betzler, C., Fürstenau, J., Lüdmann, T., Hübscher, C., Lindhorst, S., Paul, A., Reijmer, J.J.G., Droxler, A.W., 2013a. Sea-level and ocean-current control on carbonate-platform growth, Maldives, Indian Ocean. Basin Res. 25, 172–196. https://doi.org/10.1111/j.1365-2117.2012.00554.x

Betzler, C., Hübscher, C., Lindhorst, S., Reijmer, J.J.G., Römer, M., Droxler, A.W., Fürstenau, J., Lüdmann, T., 2009. Monsoon-induced partial carbonate platform drowning (Maldives, Indian Ocean). Geology 37, 867–870. https://doi.org/10.1130/G25702A.1

Betzler, C., Lüdmann, T., Hübscher, C., Fürstenau, J., 2013b. Current and sea-level signals in periplatform ooze (Neogene, Maldives, Indian Ocean). Sediment. Geol. 290, 126–137. https://doi.org/10.1016/j.sedgeo.2013.03.011

Bialik, O.M., Auer, G., Ogawa, N.O., Kroon, D., Waldmann, N.D., Ohkouchi, N., 2020. Monsoons, Upwelling, and the Deoxygenation of the Northwestern Indian Ocean in Response to Middle to Late Miocene Global Climatic Shifts. Paleoceanogr. Paleoclimatology 35, e2019PA003762. https://doi.org/10.1029/2019PA003762

Bloemsma, M., Zabel, M., Stuut, J.-B., Tjallingii, R., Collins, J., Weltje, G., 2012. Modelling the joint variability of grain size and chemical composition in sediments. Sediment. Geol. 280, 135–148. https://doi.org/10.1016/j.sedgeo.2012.04.009

Boardman, M.R., Neumann, A.C., Baker, P.A., Dulin, L.A., Kenter, R.J., Hunter, G.E., Kiefer, K.B., 1986. Banktop responses to Quaternary fluctuations in sea level recorded in periplatform sediments. Geology 14, 28–31. https://doi.org/10.1130/0091-7613(1986)14<28:BRTQFI>2.0.CO;2

Boos, W.R., Kuang, Z., 2010. Dominant control of the South Asian monsoon by orographic insulation versus plateau heating. Nature 463, 218–222. https://doi.org/10.1038/nature08707

Bosmans, J.H.C., Hilgen, F.J., Tuenter, E., Lourens, L.J., 2015. Obliquity forcing of low-latitude climate. Clim. Past 11, 1335–1346. https://doi.org/10.5194/cp-11-1335-2015

Bunzel, D., Schmiedl, G., Lindhorst, S., Mackensen, A., Reolid, J., Romahn, S., Betzler, C., 2017. A multi-proxy analysis of Late Quaternary ocean and climate variability for the Maldives, Inner Sea. Clim. Past 13, 1791–1813. https://doi.org/10.5194/cp-13-1791-2017

Calvert, S., Pedersen, T., 2007. Chapter Fourteen Elemental Proxies for Palaeoclimatic and Palaeoceanographic Variability in Marine Sediments: Interpretation and Application 1. https://doi.org/10.1016/S1572-5480(07)01019-6

Campos, E., Gonçalves, J., Ikeda, Y., 1995. Erratum: ``Water mass characteristics and geostrophic circulation in the South Brazil Bight: Summer of 1991'' [Journal of Geophysical Research, 100, 18,537-18550 (1995)]. J. Geophys. Res. 100, 22765. https://doi.org/10.1029/95JC03186

Campos, E.J.D., Velhote, D., da Silveira, I.C.A., 2000. Shelf break upwelling driven by Brazil Current Cyclonic Meanders. Geophys. Res. Lett. 27, 751–754. https://doi.org/10.1029/1999GL010502

Carrasqueira, I.G. da F., Jovane, L., Droxler, A.W., Alvarez Zarikian, C.A., Lanci, L., Alonso-Garcia, M., Laya, J.C., Kroon, D., 2023. Anomalous widespread arid events in Asia over the past 550,000 years. PNAS Nexus pgad175. https://doi.org/10.1093/pnasnexus/pgad175

Chen, G.-S., Liu, Z., Kutzbach, J.E., 2014. Reexamining the barrier effect of the Tibetan Plateau on the South Asian summer monsoon. Clim. Past 10, 1269–1275. https://doi.org/10.5194/cp-10-1269-2014

Cheng, H., Edwards, R.L., Broecker, W.S., Denton, G.H., Kong, X., Wang, Y., Zhang, R., Wang, X., 2009. Ice Age Terminations. Science 326, 248–252. https://doi.org/10.1126/science.1177840

Cheng, H., Edwards, R.L., Sinha, A., Spötl, C., Yi, L., Chen, S., Kelly, M., Kathayat, G., Wang, X., Li, X., Kong, X., Wang, Y., Ning, Y., Zhang, H., 2016. The Asian monsoon over the past 640,000 years and ice age terminations. Nature 534, 640–646. https://doi.org/10.1038/nature18591

Cheng, H., Zhang, H., Cai, Y., Shi, Z., Yi, L., Deng, C., Hao, Q., Peng, Y., Sinha, A., Li, H., Zhao, J., Tian, Y., Baker, J., Perez-Mejías, C., 2021. Orbital-scale Asian summer monsoon variations: Paradox and exploration. Sci. China Earth Sci. 64, 529–544. https://doi.org/10.1007/s11430-020-9720-y

Chiessi, C.M., Mulitza, S., Pätzold, J., Wefer, G., Marengo, J.A., 2009. Possible impact of the Atlantic Multidecadal Oscillation on the South American summer monsoon. Geophys. Res. Lett. 36. https://doi.org/10.1029/2009GL039914

Christensen, J.H., Kanikicharla, K.K., Aldrian, E., An, S.I., Albuquerque Cavalcanti, I.F., de Castro, M., Dong, W., Goswami, P., Hall, A., Kanyanga, J.K., Kitoh, A., Kossin, J., Lau, N.C., Renwick, J., Stephenson, D.B., Xie, S.P., Zhou, T., Abraham, L., Ambrizzi, T., Anderson, B., Arakawa, O., Arritt, R., Baldwin, M., Barlow, M., Barriopedro, D., Biasutti, M., Biner, S., Bromwich, D., Brown, J., Cai, W., Carvalho, L.V., Chang, P., Chen, X., Choi, J., Christensen, O.B., Deser, C., Emanuel, K., Endo, H., Enfield, D.B., Evan, A., Giannini, A., Gillett, N., Hariharasubramanian, A., Huang, P., Jones, J., Karumuri, A., Katzfey, J., Kjellström, E., Knight, J., Knutson, T., Kulkarni, A., Kundeti, K.R., Lau, W.K., Lenderink, G., Lennard, C., Leung, L. yung R., Lin, R., Losada, T., Mackellar, N.C., Magaña, V., Marshall, G., Mearns, L., Meehl, G., Menéndez, C., Murakami, H., Nath, M.J., Neelin, J.D., van Oldenborgh, G.J., Olesen, M., Polcher, J., Qian, Y., Ray, S., Reich, K.D., de Fonseca, B.R., Ruti, P., Screen, J., Sedláček, J., Solman, S., Stendel, M., Stevenson, S., Takayabu, I., Turner, J., Ummenhofer, C., Walsh, K., Wang, B., Wang, C., Watterson, I., Widlansky, M., Wittenberg, A., Woollings, T., Yeh, S.W., Zhang, C., Zhang, L., Zheng, X., Zou, L., 2013. Climate phenomena and their relevance for future regional climate change, in: Climate Change 2013 the Physical Science Basis. Cambridge University Press, pp. 1217–1308. https://doi.org/10.1017/CBO9781107415324.028

Clemens, S., 1998. Dust response to seasonal atmospheric forcing: Proxy evaluation and calibration. Paleoceanography 13. https://doi.org/10.1029/98PA02131

Clemens, S., Prell, W., Murray, D., Shimmield, G., Weedon, G., 1991. Forcing mechanisms of the Indian Ocean monsoon. Nature 353, 720–725. https://doi.org/10.1038/353720a0

Clift, P.D., Hodges, K.V., Heslop, D., Hannigan, R., Van Long, H., Calves, G., 2008. Correlation of Himalayan exhumation rates and Asian monsoon intensity. Nat. Geosci. 1, 875–880. https://doi.org/10.1038/ngeo351

Cruz, F.W., Burns, S.J., Karmann, I., Sharp, W.D., Vuille, M., Cardoso, A.O., Ferrari, J.A., Silva Dias, P.L., Viana, O., 2005. Insolation-driven changes in atmospheric circulation over the past 116,000 years in subtropical Brazil. Nature 434, 63–66. https://doi.org/10.1038/nature03365

CURRAY, J.R., MOORE, D.G., 1971. Growth of the Bengal Deep-Sea Fan and Denudation in the Himalayas. GSA Bull. 82, 563–572. https://doi.org/10.1130/0016-7606(1971)82[563:GOTBDF]2.0.CO;2

Day, R., Fuller, M., Schmidt, V.A., 1977. Hysteresis properties of titanomagnetites: Grain-size and compositional dependence. Phys. Earth Planet. Inter. 13, 260–267. https://doi.org/10.1016/0031-9201(77)90108-X

Mahiques, M.M., Mishima, Y., Rodrigues, M., 1999. Characteristics of the sedimentary organic matter on the inner and middle continental shelf between Guanabara Bay and São Francisco do Sul, southeastern Brazilian margin. Cont. Shelf Res. 19, 775–798. https://doi.org/10.1016/S0278-4343(98)00105-8

Mahiques, M.M., Tessler, M.G., Maria Ciotti, A., da Silveira, I.C.A., e Sousa, S.H. de M., Figueira, R.C.L., Tassinari, C.C.G., Furtado, V.V., Passos, R.F., 2004. Hydrodynamically driven patterns of recent sedimentation in the shelf and upper slope off Southeast Brazil. Cont. Shelf Res. 24, 1685–1697. https://doi.org/10.1016/j.csr.2004.05.013

de Oliveira, M.T.G., Formoso, M.L.L., da Costa, M.I., Meunier, A., 2002. The titanomagnetite to titanomaghemite conversion in a weathered basalt profile from southern Paraná Basin, Brazil. Clays Clay Miner. 50, 478–493. https://doi.org/10.1346/000986002320514208

Dekkers, M.J., Passier, H.F., Schoonen, M.A.A., 2000. Magnetic properties of hydrothermally synthesized greigite (Fe3S4)—II. High- and low-temperature characteristics. Geophys. J. Int. 141, 809–819. https://doi.org/10.1046/j.1365-246x.2000.00129.x

Denton, G., Anderson, R., Toggweiler, J.R., Edwards, R., Schaefer, J., Putnam, A., 2010. The Last Glacial Termination. Science 328, 1652–6. https://doi.org/10.1126/science.1184119

Depetris, P.J., Probst, J.-L., Pasquini, A.I., Gaiero, D.M., 2003. The geochemical characteristics of the Paraná River suspended sediment load: an initial assessment. Hydrol. Process. 17, 1267–1277. https://doi.org/10.1002/hyp.1283

Dias, G.P., 2018. Avaliação das condições redox das águas intermediárias do Oceano Atlântico Sudoeste nos últimos 40 mil anos (text). Universidade de São Paulo. https://doi.org/10.11606/D.21.2019.tde-29012019-163323

Droxler, A., 1990. Pliocene-Pleistocene Aragonite Cyclic Variations in Holes 714A and 716B (the Maldives) Compared with Hole 633A (the Bahamas): Records of Climate-Induced CaCO3 Preservation at Intermediate Water Depths. Proc. Ocean Drill. Program.

Droxler, A.W., Schlager, W., Whallon, C.C., 1983. Quaternary aragonite cycles and oxygen-isotope record in Bahamian carbonate ooze. Geology 11, 235. https://doi.org/10.1130/0091-7613(1983)11<235:QACAOR>2.0.CO;2

Emeis, K.-C., Anderson, D.M., Doose, H., Kroon, D., Schulz-Bull, D., 1995. Sea-Surface Temperatures and the History of Monsoon Upwelling in the Northwest Arabian Sea during the Last 500,000 Years. Quat. Res. 43, 355–361. https://doi.org/10.1006/qres.1995.1041

Emiroğlu, S., Rey, D., Petersen, N., 2004. Magnetic properties of sediment in the Ría de Arousa (Spain): dissolution of iron oxides and formation of iron sulphides. Phys. Chem. Earth

Parts ABC, Paleo, Rock and Environmental Magnetism 29, 947–959. https://doi.org/10.1016/j.pce.2004.03.012

Florindo, F., Sagnotti, L., 1995. Palaeomagnetism and rock magnetism in the upper Pliocene Valle Ricca (Rome, Italy) section. Geophys. J. Int. 123, 340–354. https://doi.org/10.1111/j.1365-246X.1995.tb06858.x

Frederichs, T., Bleil, U., Däumler, K., von Dobeneck, T., Schmidt, A.M., 1999. The Magnetic View on the Marine Paleoenvironment: Parameters, Techniques and Potentials of Rock Magnetic Studies as a Key to Paleoclimatic and Paleoceanographic Changes, in: Fischer, G., Wefer, G. (Eds.), Use of Proxies in Paleoceanography: Examples from the South Atlantic. Springer, Berlin, Heidelberg, pp. 575–599. https://doi.org/10.1007/978-3-642-58646-0_24

Fürstenau, J., Lindhorst, S., Betzler, C., Hübscher, C., 2010. Submerged reef terraces of the Maldives (Indian Ocean). Geo-Mar. Lett. 30, 511–515. https://doi.org/10.1007/s00367-009-0174-2

Furtado, V.V., Bonetti, J., Conti, L., 1996. Paleo river valley morphology and sea level changes at southeastern Brazilian continental shelf 68, 167–169.

Gaiero, D.M., Brunet, F., Probst, J.-L., Depetris, P.J., 2007. A uniform isotopic and chemical signature of dust exported from Patagonia: Rock sources and occurrence in southern environments. Chem. Geol. 238, 107–120. https://doi.org/10.1016/j.chemgeo.2006.11.003

Gaiero, D.M., Probst, J.-L., Depetris, P.J., Bidart, S.M., Leleyter, L., 2003. Iron and other transition metals in Patagonian riverborne and windborne materials: geochemical control and transport to the southern South Atlantic Ocean. Geochim. Cosmochim. Acta 67, 3603–3623. https://doi.org/10.1016/S0016-7037(03)00211-4

Galy, A., France-Lanord, C., 2001. Higher erosion rates in the Himalaya: Geochemical constraints on riverine fluxes. Geology 29, 23. https://doi.org/10.1130/0091-7613(2001)029<0023:HERITH>2.0.CO;2

Gan, M.A., Kousky, V.E., Ropelewski, C.F., 2004. The South America Monsoon Circulation and Its Relationship to Rainfall over West-Central Brazil. J. Clim. 17, 47–66. https://doi.org/10.1175/1520-0442(2004)017<0047:TSAMCA>2.0.CO;2

Garming, J.F.L., Bleil, U., Riedinger, N., 2005. Alteration of magnetic mineralogy at the sulfate–methane transition: Analysis of sediments from the Argentine continental slope. Phys. Earth Planet. Inter. 151, 290–308. https://doi.org/10.1016/j.pepi.2005.04.001

Garming, J.F.L., Von Dobeneck, T., Franke, C., Bleil, U., 2007. Low-temperature partial magnetic self-reversal in marine sediments by magnetostatic interaction of titanomagnetite and titanohematite intergrowths. Geophys. J. Int. 170, 1067–1075. https://doi.org/10.1111/j.1365-246X.2007.03504.x

Garreaud, R.D., Vuille, M., Compagnucci, R., Marengo, J., 2009. Present-day South American climate. Palaeogeogr. Palaeoclimatol. Palaeoecol., Long-term multi-proxy climate reconstructions and dynamics in South America (LOTRED-SA): State of the art and perspectives 281, 180–195. https://doi.org/10.1016/j.palaeo.2007.10.032

Gartner, S., 1990. Neogene Calcareous Nannofossil Biostratigraphy, Leg 116 (Central Indian Ocean).

Gornitz, V., 2021. Timescales of Climate Change, in: Alderton, D., Elias, S.A. (Eds.), Encyclopedia of Geology (Second Edition). Academic Press, Oxford, pp. 318–327. https://doi.org/10.1016/B978-0-08-102908-4.00107-7

Govin, A., Holzwarth, U., Heslop, D., Ford Keeling, L., Zabel, M., Mulitza, S., Collins, J.A., Chiessi, C.M., 2012. Distribution of major elements in Atlantic surface sediments (36°N-49°S): Imprint of terrigenous input and continental weathering: ATLANTIC SURFACE SEDIMENT COMPOSITION. Geochem. Geophys. Geosystems 13, n/a-n/a. https://doi.org/10.1029/2011GC003785

Guo, Z.T., Ruddiman, W.F., Hao, Q.Z., Wu, H.B., Qiao, Y.S., Zhu, R.X., Peng, S.Z., Wei, J.J., Yuan, B.Y., Liu, T.S., 2002. Onset of Asian desertification by 22 Myr ago inferred from loess deposits in China. Nature 416, 159–163. https://doi.org/10.1038/416159a

Gupta, A.K., Yuvaraja, A., Prakasam, M., Clemens, S.C., Velu, A., 2015. Evolution of the South Asian monsoon wind system since the late Middle Miocene. Palaeogeogr. Palaeoclimatol. Palaeoecol. 438, 160–167. https://doi.org/10.1016/j.palaeo.2015.08.006

Hammer, O., Harper, D.A.T., Ryan, P.D., n.d. PAST: Paleontological Statistics Software Package for Education and Data Analysis 9.

Harrison, S., Sanchez Goñi, M., 2010. Global patterns of vegetation response to millennial-scale variability and rapid climate change during the last glacial period. Quat. Sci. Rev. 29, 2957–2980. https://doi.org/10.1016/j.quascirev.2010.07.016

Hemming, S.R., 2004. Heinrich events: Massive late Pleistocene detritus layers of the North Atlantic and their global climate imprint. Rev. Geophys. 42. https://doi.org/10.1029/2003RG000128

Hilgen, F.J., Lourens, L.J., Van Dam, J.A., Beu, A.G., Boyes, A.F., Cooper, R.A., Krijgsman, W., Ogg, J.G., Piller, W.E., Wilson, D.S., 2012. Chapter 29 - The Neogene Period, in: Gradstein, F.M., Ogg, James G., Schmitz, M.D., Ogg, G.M. (Eds.), The Geologic Time Scale. Elsevier, Boston, pp. 923–978. https://doi.org/10.1016/B978-0-444-59425-9.00029-9

Holbourn, A., Kuhnt, W., Clemens, S., Prell, W., Andersen, N., 2013. Middle to late Miocene stepwise climate cooling: Evidence from a high-resolution deep water isotope curve spanning 8 million years. Paleoceanography 28, 688–699. https://doi.org/10.1002/2013PA002538

Housen, B.A., Banerjee, S.K., Moskowitz, B.M., 1996. Low-temperature magnetic properties of siderite and magnetite in marine sediments. Geophys. Res. Lett. 23, 2843–2846. https://doi.org/10.1029/96GL01197

Hovan, S., 1995. Late Cenozoic Atmospheric Circulation Intensity and Climatic History Recorded by Eolian Deposition in the Eastern Equatorial Pacific Ocean, Leg 138 138, 615–625. https://doi.org/10.2973/odp.proc.sr.138.132.1995

Iriondo, M., Brunetto, E., Kröhling, D., 2009. Historical climatic extremes as indicators for typical scenarios of Holocene climatic periods in the Pampean plain. Palaeogeogr. Palaeoclimatol. Palaeoecol. 283, 107–119. https://doi.org/10.1016/j.palaeo.2009.09.005

Jenkins, G.M., Watts, D.G., 1969. Spectral Analysis and Its Applications. Holden-Day.

Jiang, H., Ding, Z., 2010. Eolian grain-size signature of the Sikouzi lacustrine sediments (Chinese Loess Plateau): Implications for Neogene evolution of the East-Asian winter monsoon. Geol. Soc. Am. Bull. 122, 843–854. https://doi.org/10.1130/B26583.1

Jiang, H., Ding, Z., 2008. A 20 Ma pollen record of East-Asian summer monsoon evolution from Guyuan, Ningxia, China. Palaeogeogr. Palaeoclimatol. Palaeoecol. 265, 30–38. https://doi.org/10.1016/j.palaeo.2008.04.016

Jiang, W.-T., Horng, C.-S., Roberts, A.P., Peacor, D.R., 2001. Contradictory magnetic polarities in sediments and variable timing of neoformation of authigenic greigite. Earth Planet. Sci. Lett. 193, 1–12. https://doi.org/10.1016/S0012-821X(01)00497-6

Kao, S.-J., Horng, C.-S., Roberts, A.P., Liu, K.-K., 2004. Carbon–sulfur–iron relationships in sedimentary rocks from southwestern Taiwan: influence of geochemical environment on greigite and pyrrhotite formation. Chem. Geol. 203, 153–168. https://doi.org/10.1016/j.chemgeo.2003.09.007

Kawamura, N., Oda, H., Ikehara, K., Yamazaki, T., Shioi, K., Taga, S., Hatakeyama, S., Torii, M., 2007. Diagenetic effect on magnetic properties of marine core sediments from the southern Okhotsk Sea. Earth Planets Space 59, 83–93. https://doi.org/10.1186/BF03352680

Kent, J.T., 1982. The Fisher-Bingham Distribution on the Sphere. J. R. Stat. Soc. Ser. B Methodol. 44, 71–80.

Kessarkar, P.M., Rao, V.P., Ahmad, S.M., Babu, G.A., 2003. Clay minerals and Sr–Nd isotopes of the sediments along the western margin of India and their implication for sediment provenance. Mar. Geol. 202, 55–69. https://doi.org/10.1016/S0025-3227(03)00240-8

Kido, Y., Koshikawa, T., Tada, R., 2006. Rapid and quantitative major element analysis method for wet fine-grained sediments using an XRF microscanner. Mar. Geol. 229, 209–225. https://doi.org/10.1016/j.margeo.2006.03.002

King, J., Banerjee, S.K., Marvin, J., Özdemir, Ö., 1982. A comparison of different magnetic methods for determining the relative grain size of magnetite in natural materials: Some results from lake sediments. Earth Planet. Sci. Lett. 59, 404–419. https://doi.org/10.1016/0012-821X(82)90142-X

Kirschvink, J.L., 1980. The least-squares line and plane and the analysis of palaeomagnetic data. Geophys. J. Int. 62, 699–718. https://doi.org/10.1111/j.1365-246X.1980.tb02601.x

Kolla, V., Coumes, F., 1987. Morphology, Internal Structure, Seismic Stratigraphy, and Sedimentation of Indus Fan. AAPG Bull. 71, 650–677.

Kramer, P., Swart, P., De, E., Schovsbo, N., 2000. Overview of interstitial fluid and sediment geochemistry, Sites 1003-1007 (Bahamas Transect). Proc. Ocean Drill. Program Sci. Results 166, 1003–1007. https://doi.org/10.2973/odp.proc.sr.166.117.2000

Kroon, D., Steens, T., Troelstra, S., 1991. Onset of Monsoonal Related Upwelling in the Western Arabian Sea as Revealed by Planktonic Foraminifers. Proc. Ocean Drill. Program Sci. Results 117, 257–263. https://doi.org/10.2973/odp.proc.sr.117.126.1991

Krs, M., Novák, F., Krsová, M., Pruner, P., Kouklíková, L., Jansa, J., 1992. Magnetic properties and metastability of greigite-smythite mineralization in brown-coal basins of the Krušné hory Piedmont, Bohemia. Phys. Earth Planet. Inter. 70, 273–287. https://doi.org/10.1016/0031-9201(92)90194-Z

Kumar, A., Sudheer, A.K., Sarin, M.M., 2008. Chemical characteristics of aerosols in MABL of Bay of Bengal and Arabian Sea during spring inter-monsoon: A comparative study. J. Earth Syst. Sci. 117, 325–332. https://doi.org/10.1007/s12040-008-0035-9

Kumar, A., Suresh, K., Rahaman, W., 2020. Geochemical characterization of modern aeolian dust over the Northeastern Arabian Sea: Implication for dust transport in the Arabian Sea. Sci. Total Environ. 729, 138576. https://doi.org/10.1016/j.scitotenv.2020.138576

Kunkelova, T., Jung, S.J.A., de Leau, E.S., Odling, N., Thomas, A.L., Betzler, C., Eberli, G.P., Alvarez-Zarikian, C.A., Alonso-García, M., Bialik, O.M., Blättler, C.L., Guo, J.A., Haffen, S., Horozal, S., Mee, A.L.H., Inoue, M., Jovane, L., Lanci, L., Laya, J.C., Lüdmann, T., Bejugam, N.N., Nakakuni, M., Niino, K., Petruny, L.M., Pratiwi, S.D., Reijmer, J.J.G., Reolid, J., Slagle, A.L., Sloss, C.R., Su, X., Swart, P.K., Wright, J.D., Yao, Z., Young, J.R., Lindhorst, S., Stainbank, S., Rueggeberg, A., Spezzaferri, S., Carrasqueira, I., Yu, S., Kroon, D., 2018. A two million year record of low-latitude aridity linked to continental weathering from the Maldives. Prog. Earth Planet. Sci. 5, 86. https://doi.org/10.1186/s40645-018-0238-x

Kurian, J., Vinayachandran, P.N., 2007. Mechanisms of formation of the Arabian Sea mini warm pool in a high-resolution Ocean General Circulation Model. J. Geophys. Res. Oceans 112. https://doi.org/10.1029/2006JC003631

L3 Browser - NASA Ocean Color [WWW Document], n.d. URL https://oceancolor.gsfc.nasa.gov/l3/ (accessed 6.28.22).

Lachkar, Z., Lévy, M., Smith, S., 2018. Intensification and deepening of the Arabian Sea oxygen minimum zone in response to increase in Indian monsoon wind intensity. Biogeosciences 15, 159–186. https://doi.org/10.5194/bg-15-159-2018

Lahiri, S.P., Vissa, N.K., 2022. Assessment of Indian Ocean upwelling changes and its relationship with the Indian monsoon. Glob. Planet. Change 208, 103729. https://doi.org/10.1016/j.gloplacha.2021.103729

Lanci, L., Zanella, E., Jovane, L., Galeotti, S., Alonso-García, M., Alvarez-Zarikian, C.A., Bejugam, N.N., Betzler, C., Bialik, O.M., Blättler, C.L., Eberli, G.P., Guo, J.A., Haffen, S., Horozal, S., Inoue, M., Kroon, D., Laya, J.C., Mee, A.L.H., Lüdmann, T., Nakakuni, M., Niino, K., Petruny, L.M., Pratiwi, S.D., Reijmer, J.J.G., Reolid, J., Slagle, A.L., Sloss, C.R., Su, X., Swart, P.K., Wright, J.D., Yao, Z., Young, J.R., 2019. Magnetic properties of early Pliocene sediments from IODP Site U1467 (Maldives platform) reveal changes in the monsoon system. Palaeogeogr. Palaeoclimatol. Palaeoecol. 533, 109283. https://doi.org/10.1016/j.palaeo.2019.109283

Laprida, C., Chapori, N.G., Violante, R.A., Compagnucci, R.H., 2007. Mid-Holocene evolution and paleoenvironments of the shoreface–offshore transition, north-eastern Argentina: New evidence based on benthic microfauna. Mar. Geol. 240, 43–56. https://doi.org/10.1016/j.margeo.2007.02.001

Laskar, J., Fienga, A., Gastineau, M., Manche, H., 2011. La2010: a new orbital solution for the long-term motion of the Earth. Astron. Astrophys. 532, A89. https://doi.org/10.1051/0004-6361/201116836

Laskar, J., Robutel, P., Joutel, F., Gastineau, M., Correia, A.C.M., Levrard, B., 2004. A long-term numerical solution for the insolation quantities of the Earth. Astron. Astrophys. 428, 261–285. https://doi.org/10.1051/0004-6361:20041335

Laskin, A., Laskin, J., Nizkorodov, S.A., 2015. Chemistry of Atmospheric Brown Carbon. Chem. Rev. 115, 4335–4382. https://doi.org/10.1021/cr5006167

Levine, R.C., Turner, A.G., 2012. Dependence of Indian monsoon rainfall on moisture fluxes across the Arabian Sea and the impact of coupled model sea surface temperature biases. Clim. Dyn. 38, 2167–2190. https://doi.org/10.1007/s00382-011-1096-z

Levy, R., Harwood, D., Florindo, F., Sangiorgi, F., Tripati, R., von Eynatten, H., Gasson, E., Kuhn, G., Tripati, A., DeConto, R., Fielding, C., Field, B., Golledge, N., McKay, R., Naish, T., Olney, M., Pollard, D., Schouten, S., Talarico, F., Warny, S., Willmott, V., Acton, G., Panter, K., Paulsen, T., Taviani, M., SMS Science Team, 2016. Antarctic ice sheet sensitivity to atmospheric CO2 variations in the early to mid-Miocene. Proc. Natl. Acad. Sci. 113, 3453–3458. https://doi.org/10.1073/pnas.1516030113

Li, G., Xie, S.-P., He, C., Chen, Z., 2017. Western Pacific emergent constraint lowers projected increase in Indian summer monsoon rainfall. Nat. Clim. Change 7, 708–712. https://doi.org/10.1038/nclimate3387

Li, M., Hinnov, L., Kump, L., 2019. Acycle: Time-series analysis software for paleoclimate research and education. Comput. Geosci. 127, 12–22. https://doi.org/10.1016/j.cageo.2019.02.011

Lindhorst, S., Betzler, C., Kroon, D., 2019. Wind variability over the northern Indian Ocean during the past 4 million years – insights from coarse aeolian dust (IODP Exp. 359, Site U1467, Maldives). Palaeogeogr. Palaeoclimatol. Palaeoecol. 536, 109371. https://doi.org/10.1016/j.palaeo.2019.109371

Ling, A., Eberli, G.P., Swart, P.K., Reolid, J., Stainbank, S., Rüggeberg, A., Betzler, C., 2021. Middle Miocene platform drowning in the Maldives associated with monsoon-related intensification of currents. Palaeogeogr. Palaeoclimatol. Palaeoecol. 567, 110275. https://doi.org/10.1016/j.palaeo.2021.110275

Lisiecki, L.E., Raymo, M.E., 2005. A Pliocene-Pleistocene stack of 57 globally distributed benthic δ18O records. Paleoceanography 20. https://doi.org/10.1029/2004PA001071

Liu, G., Li, X., Chiang, H.-W., Cheng, H., Yuan, S., Chawchai, S., He, S., Lu, Y., Aung, L.T., Maung, P.M., Tun, W.N., Oo, K.M., Wang, X., 2020. On the glacial-interglacial variability of the Asian monsoon in speleothem δ18O records. Sci. Adv. 6, eaay8189. https://doi.org/10.1126/sciadv.aay8189

Liu, J., Zhu, R., Roberts, A.P., Li, S., Chang, J.-H., 2004. High-resolution analysis of early diagenetic effects on magnetic minerals in post-middle-Holocene continental shelf sediments from the Korea Strait. J. Geophys. Res. Solid Earth 109. https://doi.org/10.1029/2003JB002813

Liu, Q., Roberts, A.P., Torrent, J., Horng, C.-S., Larrasoaña, J.C., 2007. What do the HIRM and *S* -ratio really measure in environmental magnetism?: *HIRM* AND *S* -RATIO MEASUREMENTS. Geochem. Geophys. Geosystems 8, n/a-n/a. https://doi.org/10.1029/2007GC001717

Lourens, L., Hilgen, F., Shackleton, N.J., Laskar, J., Wilson, D., 2005. The Neogene Period, in: Smith, A.G., Gradstein, F.M., Ogg, J.G. (Eds.), A Geologic Time Scale 2004. Cambridge University Press, Cambridge, pp. 409–440. https://doi.org/10.1017/CBO9780511536045.022

Lübbers, J., Kuhnt, W., Holbourn, A.E., Bolton, C.T., Gray, E., Usui, Y., Kochhann, K.G.D., Beil, S., Andersen, N., 2019. The Middle to Late Miocene "Carbonate Crash" in the Equatorial Indian Ocean. Paleoceanogr. Paleoclimatology 34, 813–832. https://doi.org/10.1029/2018PA003482

Lüdmann, T., Kalvelage, C., Betzler, C., Lampart, J., Huebscher, C., 2013. The Maldives, a giant isolated carbonate platform dominated by bottom currents. Mar. Pet. Geol. 43, 326–340. https://doi.org/10.1016/j.marpetgeo.2013.01.004

Lund, D.C., Tessin, A.C., Hoffman, J.L., Schmittner, A., 2015. Southwest Atlantic water mass evolution during the last deglaciation. Paleoceanography 30, 477–494. https://doi.org/10.1002/2014PA002657

Lurcock, P.C., Wilson, G.S., 2012. PuffinPlot: A versatile, user-friendly program for paleomagnetic analysis. Geochem. Geophys. Geosystems 13. https://doi.org/10.1029/2012GC004098

Maher, B., Prospero, J., Mackie, D., Gaiero, D., Hesse, P., Balkanski, Y., 2010. Global connections between aeolian dust, climate and ocean biogeochemistry at the present day and at the last glacial maximum. https://doi.org/10.1016/J.EARSCIREV.2009.12.001

Mahiques, M.M. de, Tassinari, C.C.G., Marcolini, S., Violante, R.A., Figueira, R.C.L., Silveira, I.C.A. da, Burone, L., Sousa, S.H. de M. e, 2008. Nd and Pb isotope signatures on the Southeastern South American upper margin: Implications for sediment transport and source rocks. Mar. Geol. 250, 51.

Malone, M.J., Baker, P.A., Burns, S.J., Swart, P.K., n.d. 35. GEOCHEMISTRY OF PERIPLATFORM CARBONATE SEDIMENTS, LEG 115, SITE 716 (MALDIVES ARCHIPELAGO, INDIAN OCEAN) 13.

Mathias, G., Nagai, R., Trindade, R., Mahiques, M., 2014. Magnetic fingerprint of the late Holocene inception of the Río de la Plata plume onto the southeast Brazilian shelf. Palaeogeogr. Palaeoclimatol. Palaeoecol. 415. https://doi.org/10.1016/j.palaeo.2014.03.034

Mayergoyz, I., 1986. Mathematical Models of Hysteresis. Magn. IEEE Trans. On 22, 603–608. https://doi.org/10.1109/TMAG.1986.1064347

McKay, N.P., Kaufman, D.S., Routson, C.C., Erb, M.P., Zander, P.D., 2018. The Onset and Rate of Holocene Neoglacial Cooling in the Arctic. Geophys. Res. Lett. 45, 12,487-12,496. https://doi.org/10.1029/2018GL079773

Merrill, R.T., McElhinny, M.W., McFadden, P.L., 1998. The Magnetic Field of the Earth: Paleomagnetism, the Core, and the Deep Mantle. Academic Press.

Mahiques, M., Almeida da Silveira, I.C., de Mello e Sousa, S.H., Rodrigues, M., 2002. Post-LGM sedimentation on the outer shelf–upper slope of the northernmost part of the São Paulo Bight, southeastern Brazil. Mar. Geol. 181, 387–400. https://doi.org/10.1016/S0025-3227(01)00225-0

Minyuk, P.S., Subbotnikova, T.V., Plyashkevich, A.A., 2011. Measurements of thermal magnetic susceptibility of hematite and goethite. Izv. Phys. Solid Earth 47, 762–774. https://doi.org/10.1134/S1069351311080052

Moore, E.W., Swart, P.K., 2022. Evidence for recrystallization and fluid advection in the Maldives using the sulfur isotopic composition of porewaters, carbonates, and celestine. Chem. Geol. 609, 121062. https://doi.org/10.1016/j.chemgeo.2022.121062

Moosmüller, H., Chakrabarty, R.K., Arnott, W.P., 2009. Aerosol light absorption and its measurement: A review. J. Quant. Spectrosc. Radiat. Transf., Light Scattering: Mie and More Commemorating 100 years of Mie's 1908 publication 110, 844–878. https://doi.org/10.1016/j.jqsrt.2009.02.035

Müller, T.J., Ikeda, Y., Zangenberg, N., Nonato, L.V., 1998. Direct measurements of western boundary currents off Brazil between 20°S and 28°S. J. Geophys. Res. Oceans 103, 5429–5437. https://doi.org/10.1029/97JC03529

Murty, A., 2021. Monsoons over the Indian Subcontinent. Acad. Lett.

Muxworthy, A.R., Turney, J.N., Qi, L., Baker, E.B., Perkins, J.R., Abdulkarim, M.A., 2023. Interpreting high-temperature magnetic susceptibility data of natural systems. Front. Earth Sci. 11.

Nobre, C.A., Sampaio, G., Borma, L.S., Castilla-Rubio, J.C., Silva, J.S., Cardoso, M., 2016. Land-use and climate change risks in the Amazon and the need of a novel sustainable development paradigm. Proc. Natl. Acad. Sci. 113, 10759–10768. https://doi.org/10.1073/pnas.1605516113

Ogg, J.G., 2020. Chapter 5 - Geomagnetic Polarity Time Scale, in: Gradstein, F.M., Ogg, James G., Schmitz, M.D., Ogg, G.M. (Eds.), Geologic Time Scale 2020. Elsevier, pp. 159–192. https://doi.org/10.1016/B978-0-12-824360-2.00005-X

Orgeira, M., Vasquez, C., Compagnucci, R., Raposo, I., Pereyra, F., 2009. Magnetismo de rocas en suelos actuales de la Pampa Ondulada, Provincia de Buenos Aires, Argentina: Vinculación del clima con el comportamiento magnético. Rev. Mex. Cienc. Geológicas ISSN 1026-8774 Vol 26 Nº 1 2009 Pags 65-78.

Orgeira, M.J., Pereyra, F.X., Vásquez, C., Castañeda, E., Compagnucci, R., 2008. Rock magnetism in modern soils, Buenos Aires Province, Argentina. J. South Am. Earth Sci. 26, 217–224. https://doi.org/10.1016/j.jsames.2008.03.007

OrgeIra, M.J., Walther, A.M., Vásquez, C.A., Tommaso, I.D., Alonso, S., Sherwood, G., Yuguan, H., Vilas, J.F.A., 1998. Mineral magnetic record of paleoclimate variation in loess and paleosol from the Buenos Aires formation (Buenos Aires, Argentina). J. South Am. Earth Sci. 11, 561–570. https://doi.org/10.1016/S0895-9811(98)00038-8

Paul, A., Reijmer, J., Lampart, J., Kinkel, H., Betzler, C., 2012. Relationship between Late Pleistocene sea-level variations, carbonate platform morphology and aragonite production (Maldives, Indian Ocean). Sedimentology 59, 1640–1658. https://doi.org/10.1111/j.1365-3091.2011.01319.x

Pearson, P.N., Palmer, M.R., 2000. Atmospheric carbon dioxide concentrations over the past 60 million years. Nature 406, 695–699. https://doi.org/10.1038/35021000

Piola, A.R., Campos, E.J.D., Möller Jr., O.O., Charo, M., Martinez, C., 2000. Subtropical Shelf Front off eastern South America. J. Geophys. Res. Oceans 105, 6565–6578. https://doi.org/10.1029/1999JC000300

Piola, A.R., Matano, R.P., Palma, E.D., Möller Jr., O.O., Campos, E.J.D., 2005. The influence of the Plata River discharge on the western South Atlantic shelf. Geophys. Res. Lett. 32. https://doi.org/10.1029/2004GL021638

Piola, A.R., Romero, S.I., Zajaczkovski, U., 2008. Space time variability of the Plata plume inferred from ocean color. Cont. Shelf Res. 28, 1556–1567. https://doi.org/10.1016/j.csr.2007.02.013

Poulton, S.W., Krom, M.D., Raiswell, R., 2004. A revised scheme for the reactivity of iron (oxyhydr)oxide minerals towards dissolved sulfide. Geochim. Cosmochim. Acta 68, 3703–3715. https://doi.org/10.1016/j.gca.2004.03.012

Pound, M.J., Haywood, A.M., Salzmann, U., Riding, J.B., 2012. Global vegetation dynamics and latitudinal temperature gradients during the Mid to Late Miocene (15.97–5.33Ma). Earth-Sci. Rev. 112, 1–22. https://doi.org/10.1016/j.earscirev.2012.02.005

Preiss-Daimler, I., Zarkogiannis, S.D., Kontakiotis, G., Henrich, R., Antonarakou, A., 2021. Paleoceanographic Perturbations and the Marine Carbonate System during the Middle

to Late Miocene Carbonate Crash—A Critical Review. Geosciences 11, 94. https://doi.org/10.3390/geosciences11020094

Prell, W.L., Kutzbach, J.E., 1992. Sensitivity of the Indian monsoon to forcing parameters and implications for its evolution. Nature 360, 647–652. https://doi.org/10.1038/360647a0

Prospero, J.M., Ginoux, P., Torres, O., Nicholson, S.E., Gill, T.E., 2002. Environmental Characterization of Global Sources of Atmospheric Soil Dust Identified with the Nimbus 7 Total Ozone Mapping Spectrometer (toms) Absorbing Aerosol Product. Rev. Geophys. 40, 2-1-2–31. https://doi.org/10.1029/2000RG000095

Purdy, E.G., Bertram, G.T., 1993. Carbonate Concepts from the Maldives, Indian Ocean 47, 7–55.

Qiang, X., An, Z., Song, Y., Chang, H., Sun, Y., Liu, W., Ao, H., Dong, J., Fu, C., Wu, F., Lu, F., Cai, Y., Zhou, W., Cao, J., Xu, X., Ai, L., 2011. New eolian red clay sequence on the western Chinese Loess Plateau linked to onset of Asian desertification about 25 Ma ago. Sci. China Earth Sci. 54, 136–144. https://doi.org/10.1007/s11430-010-4126-5

Razik, S., Chiessi, C.M., Romero, O.E., von Dobeneck, T., 2013. Interaction of the South American Monsoon System and the Southern Westerly Wind Belt during the last 14kyr. Palaeogeogr. Palaeoclimatol. Palaeoecol. 374, 28–40. https://doi.org/10.1016/j.palaeo.2012.12.022

Rea, D.K., 1994. The paleoclimatic record provided by eolian deposition in the deep sea: The geologic history of wind. Rev. Geophys. 32, 159–195. https://doi.org/10.1029/93RG03257

Rea, D.K., 1992. Delivery of Himalayan sediment to the northern Indian Ocean and its relation to global climate, sea level, uplift, and seawater strontium. Wash. DC Am. Geophys. Union Geophys. Monogr. Ser. 70, 387–402. https://doi.org/10.1029/GM070p0387

Reijmer, J.J.G., Bauch, T., Schäfer, P., 2012. Carbonate facies patterns in surface sediments of upwelling and non-upwelling shelf environments (Panama, East Pacific). Sedimentology 59, 32–56. https://doi.org/10.1111/j.1365-3091.2010.01214.x

Reimer, P.J., Bard, E., Bayliss, A., Beck, J.W., Blackwell, P.G., Ramsey, C.B., Buck, C.E., Cheng, H., Edwards, R.L., Friedrich, M., Grootes, P.M., Guilderson, T.P., Haflidason, H., Hajdas, I., Hatté, C., Heaton, T.J., Hoffmann, D.L., Hogg, A.G., Hughen, K.A., Kaiser, K.F., Kromer, B., Manning, S.W., Niu, M., Reimer, R.W., Richards, D.A., Scott, E.M., Southon, J.R., Staff, R.A., Turney, C.S.M., Plicht, J. van der, 2013. IntCal13 and Marine13 Radiocarbon Age Calibration Curves 0–50,000 Years cal BP. Radiocarbon 55, 1869–1887. https://doi.org/10.2458/azu_js_rc.55.16947

Rey, D., Mohamed, K.J., Bernabeu, A., Rubio, B., Vilas, F., 2005. Early diagenesis of magnetic minerals in marine transitional environments: geochemical signatures of hydrodynamic forcing. Mar. Geol. 215, 215–236. https://doi.org/10.1016/j.margeo.2004.12.001

Roberts, A.P., 2015. Magnetic mineral diagenesis. Earth-Sci. Rev. 151, 1–47. https://doi.org/10.1016/j.earscirev.2015.09.010

Roberts, A.P., Chang, L., Rowan, C.J., Horng, C.-S., Florindo, F., 2011. Magnetic properties of sedimentary greigite (Fe_3S_4): An update. Rev. Geophys. 49, RG1002. https://doi.org/10.1029/2010RG000336

Roberts, A.P., Pike, C.R., Verosub, K.L., 2000. First-order reversal curve diagrams: a new tool for characterizing the magnetic properties of natural samples. J. Geophys. Res. 105, 28461–28475. https://doi.org/10.1029/2000JB900326

Roberts, A.P., Weaver, R., 2005. Multiple mechanisms of remagnetization involving sedimentary greigite (Fe3S4). Earth Planet. Sci. Lett. 231, 263–277. https://doi.org/10.1016/j.epsl.2004.11.024

Robinson, S.G., 1986. The late Pleistocene palaeoclimatic record of North Atlantic deep-sea sediments revealed by mineral-magnetic measurements. Phys. Earth Planet. Inter., Physics of the earth and planetary interiors 42, 22–47. https://doi.org/10.1016/S0031-9201(86)80006-1

Robinson, S.G., Sahota, J.T.S., Oldfield, F., 2000. Early diagenesis in North Atlantic abyssal plain sediments characterized by rock-magnetic and geochemical indices. Mar. Geol. 163, 77–107. https://doi.org/10.1016/S0025-3227(99)00108-5

Rodelli, D., Jovane, L., Giorgioni, M., Siciliano Rego, E., Cornaggia, F., Benites, M., Padua, P., Berbel, G., Braga, E., Ustra, A., Abreu, F., Roberts, A., 2019. Diagenetic Fate of Biogenic Soft and Hard Magnetite in Chemically Stratified Sedimentary Environments of Mamanguá Ría, Brazil. J. Geophys. Res. Solid Earth 124. https://doi.org/10.1029/2018JB016576

Rodelli, D., Jovane, L., Roberts, A. p., Cypriano, J., Abreu, F., Lins, U., 2018. Fingerprints of partial oxidation of biogenic magnetite from cultivated and natural marine magnetotactic bacteria using synchrotron radiation. Environ. Microbiol. Rep. 10, 337–343. https://doi.org/10.1111/1758-2229.12644

Rodríguez-Zorro, P.A., Ledru, M.-P., Bard, E., Aquino-Alfonso, O., Camejo, A., Daniau, A.-L., Favier, C., Garcia, M., Mineli, T.D., Rostek, F., Ricardi-Branco, F., Sawakuchi, A.O., Simon, Q., Tachikawa, K., Thouveny, N., 2020. Shut down of the South American summer monsoon during the penultimate glacial. Sci. Rep. 10, 6275. https://doi.org/10.1038/s41598-020-62888-x

Röhl, U., Abrams, L., 2000. High-resolution, downhole, and nondestructive core measurements from Sites 999 and 1001 in the Caribbean Sea: Application to the Late Paleocene Thermal Maximum. Proc. Ocean Drill. Program Sci. Results 165, 191–203. https://doi.org/10.2973/odp.proc.sr.165.009.2000

Rostek, F., Bard, E., Beaufort, L., Sonzogni, C., Ganssen, G., 1997. Sea surface temperature and productivity records for the past 240 kyr in the Arabian Sea. Deep Sea Res. Part II Top. Stud. Oceanogr. 44, 1461–1480. https://doi.org/10.1016/S0967-0645(97)00008-8

Rowan, C.J., Roberts, A.P., 2006. Magnetite dissolution, diachronous greigite formation, and secondary magnetizations from pyrite oxidation: Unravelling complex magnetizations in Neogene marine sediments from New Zealand. Earth Planet. Sci. Lett. 241, 119–137. https://doi.org/10.1016/j.epsl.2005.10.017

Rowan, C.J., Roberts, A.P., Broadbent, T., 2009. Reductive diagenesis, magnetite dissolution, greigite growth and paleomagnetic smoothing in marine sediments: A new view. Earth Planet. Sci. Lett. 277, 223–235. https://doi.org/10.1016/j.epsl.2008.10.016

Roxy, M.K., Ghosh, S., Pathak, A., Athulya, R., Mujumdar, M., Murtugudde, R., Terray, P., Rajeevan, M., 2017. A threefold rise in widespread extreme rain events over central India. Nat. Commun. 8, 708. https://doi.org/10.1038/s41467-017-00744-9

Russell, P.B., Bergstrom, R.W., Shinozuka, Y., Clarke, A.D., DeCarlo, P.F., Jimenez, J.L., Livingston, J.M., Redemann, J., Dubovik, O., Strawa, A., 2010. Absorption Angstrom Exponent in AERONET and related data as an indicator of aerosol composition. Atmospheric Chem. Phys. 10, 1155–1169. https://doi.org/10.5194/acp-10-1155-2010

Sagnotti, L., Roberts, A.P., Weaver, R., Verosub, K.L., Florindo, F., Pike, C.R., Clayton, T., Wilson, G.S., 2005. Apparent magnetic polarity reversals due to remagnetization resulting from late diagenetic growth of greigite from siderite. Geophys. J. Int. 160, 89–100. https://doi.org/10.1111/j.1365-246X.2005.02485.x

Sarkar, S., Kafatos, M., 2004. Interannual variability of vegetation over the Indian sub-continent and its relation to the different meteorological parameters. Remote Sens. Environ. 90, 268–280. https://doi.org/10.1016/j.rse.2004.01.003

Schiller, A., Godfrey, J.S., 2003. Indian Ocean Intraseasonal Variability in an Ocean General Circulation Model. J. Clim. 16, 21–39. https://doi.org/10.1175/1520-0442(2003)016<0021:IOIVIA>2.0.CO;2

Schmid, C., Siedler, G., Zenk, W., 2000. Dynamics of Intermediate Water Circulation in the Subtropical South Atlantic. J. Phys. Oceanogr. - J PHYS Ocean. 30, 3191–3211. https://doi.org/10.1175/1520-0485(2000)030<3191:DOIWCI>2.0.CO;2

Schneider, D., 1988. Inclination anomalies from Indian Ocean sediments and the possibility of a standing nondipole field. J. Geophys. Res. Solid Earth 931, 11621–11630. https://doi.org/10.1029/JB093iB10p11621

Schneider, D.A., Kent, D.V., 1988. The Paleomagnetic Field from Equatorial Deep-Sea Sediments: Axial Symmetry and Polarity Asymmetry. Science 242, 252–256. https://doi.org/10.1126/science.242.4876.252

Shetye, S.R., Gouveia, A.D., Shankar, D., Shenoi, S.S.C., Vinayachandran, P.N., Sundar, D., Michael, G.S., Nampoothiri, G., 1996. Hydrography and circulation in the western Bay of Bengal during the northeast monsoon.

Skinner, B.J., Erd, R.C., Grimaldi, F.S., 1964. Greigite, the thio-spinel of iron; a new mineral. Am. Mineral. 49, 543–555.

Song, Chunhui, Hu, Sihu, Han, Wenxia, Zhang, Tao, Fang, Xiaomin, Gao, Junping, Wu, Fuli, Song, C., Hu, S., Han, W., Zhang, T., Fang, X., Gao, J., Wu, F., 2014. Middle Miocene to earliest Pliocene sedimentological and geochemical records of climate change in the western Qaidam Basin on the NE Tibetan Plateau. Palaeogeogr. Palaeoclimatol. Palaeoecol. Complete, 67–76. https://doi.org/10.1016/j.palaeo.2013.12.022

Sreevidya, E., Sijinkumar, A.V., Bejugam, N., 2019. Aragonite pteropod abundance and preservation records from the Maldives, equatorial Indian Ocean: Inferences on past oceanic carbonate saturation and dissolution events. Palaeogeogr. Palaeoclimatol. Palaeoecol. 534, 109313. https://doi.org/10.1016/j.palaeo.2019.109313

Stainbank, S., Spezzaferri, S., De Boever, E., Bouvier, A.-S., Chilcott, C., de Leau, E.S., Foubert, A., Kunkelova, T., Pichevin, L., Raddatz, J., Rüggeberg, A., Wright, J.D., Yu, S.M., Zhang, M., Kroon, D., 2020. Long-term, high-resolution foraminiferal geochemical records ($\delta^{18}O$, $\delta^{13}C$) from IODP Site 359-U1467. https://doi.org/10.1594/PANGAEA.914883

Stainbank, S., Spezzaferri, S., Rüggeberg, A., Raddatz, J., de Leau, E., Yu, S., Zhang, M., Kroon, D., 2021. Monsoon and tropical climate forcing on the physicochemical and thermocline characteristics of the Maldives Inner Sea: Insights from Marine Isotope Stages 1 – 2 and 10 – 13. Paleoceanogr. Paleoclimatology 36. https://doi.org/10.1029/2020PA004105

Steffensen, J.P., Andersen, K.K., Bigler, M., Clausen, H.B., Dahl-Jensen, D., Fischer, H., Goto-Azuma, K., Hansson, M., Johnsen, S.J., Jouzel, J., Masson-Delmotte, V., Popp, T., Rasmussen, S.O., Röthlisberger, R., Ruth, U., Stauffer, B., Siggaard-Andersen, M.-L., Sveinbjörnsdóttir, A.E., Svensson, A., White, J.W.C., 2008. High-Resolution Greenland

Ice Core Data Show Abrupt Climate Change Happens in Few Years. Science 321, 680–684.

Stramma, L., England, M., 1999. On the water masses and mean circulation of the South Atlantic Ocean. J. Geophys. Res. Oceans 104, 20863–20883. https://doi.org/10.1029/1999JC900139

Swart, P., 2000. The oxygen isotopic composition of interstitial waters: Evidence for fluid flow and recrystallization in the margin of the Great Bahama Bank. Proc. Ocean Drill. Program Sci. Results 166. https://doi.org/10.2973/odp.proc.sr.166.130.2000

Tada, R., Zheng, H., Clift, P.D., 2016. Evolution and variability of the Asian monsoon and its potential linkage with uplift of the Himalaya and Tibetan Plateau. Prog. Earth Planet. Sci. 3, 4. https://doi.org/10.1186/s40645-016-0080-y

Tamrat, E., Ernesto, M., 1999. Magnetic fabric and rock-magnetic character of the Mesozoic flood basalts of the Paraná Basin, Brazil. J. Geodyn. 28, 419–437. https://doi.org/10.1016/S0264-3707(99)00019-8

Terminiello, L., Bidegain, J.C., Rico, Y., Mercader, R.C., 2001. Characterization of Argentine Loess and Paleosols by Mössbauer Spectroscopy. Hyperfine Interact. 136, 97–104. https://doi.org/10.1023/A:1015503410451

Thiry, M., 2000. Palaeoclimatic interpretation of clay minerals in marine deposits: an outlook from the continental origin. Earth-Sci. Rev. 49, 201–221. https://doi.org/10.1016/S0012-8252(99)00054-9

Thomson, D.J., 1982. Spectrum estimation and harmonic analysis.

Till, J.L., Nowaczyk, N., 2018. Authigenic magnetite formation from goethite and hematite and chemical remanent magnetization acquisition. Geophys. J. Int. 213, 1818–1831. https://doi.org/10.1093/gji/ggy083

Tjallingii, R., Röhl, U., Kölling, M., Bickert, T., 2007. Influence of the water content on X-ray fluorescence core-scanning measurements in soft marine sediments. Geochem. Geophys. Geosystems 8. https://doi.org/10.1029/2006GC001393

Torii, M., Fukuma, K., Horng, C.-S., Lee, T.-Q., 1996. Magnetic discrimination of pyrrhotite- and greigite-bearing sediment samples. Geophys. Res. Lett. 23, 1813–1816. https://doi.org/10.1029/96GL01626

Torsvik, T.H., Van Der Voo, R., Preeden, U., Mac Niocaill, C., Steinberger, B., Doubrovine, P.V., Van Hinsbergen, D.J.J., Domeier, M., Gaina, C., Tohver, E., Meert, J.G., Mccausland, P.J.A., Cocks, L.R.M., 2012. Phanerozoic polar wander, palaeogeography and dynamics. Earth-Sci. Rev. 114, 325–368. https://doi.org/10.1016/j.earscirev.2012.06.007

Vera, C., Vigliarolo, P., Berbery, E., 2002. Cold Season Synoptic-Scale Waves over Subtropical South America. Mon. Weather Rev. - MON WEATHER REV 130. https://doi.org/10.1175/1520-0493(2002)130<0684:CSSSWO>2.0.CO;2

Vernekar, A.D., Zhou, J., Shukla, J., 1995. The Effect of Eurasian Snow Cover on the Indian Monsoon. J. Clim. 8, 248–266. https://doi.org/10.1175/1520-0442(1995)008<0248:TEOESC>2.0.CO;2

Wasilewski, P.J., 1973. Magnetic hysteresis in natural materials. Earth Planet. Sci. Lett. 20, 67–72. https://doi.org/10.1016/0012-821X(73)90140-4

Weldeab, S., Schneider, R.R., Koelling, M., 2006. Deglacial sea surface temperature and salinity increase in the western tropical Atlantic in synchrony with high latitude climate

instabilities. Earth Planet. Sci. Lett. 241, 699–706. https://doi.org/10.1016/j.epsl.2005.11.012

Weltje, G., Tjallingii, R., 2008. Calibration of XRF core scanners for quantitative geochemical logging of sediment cores: Theory and application. Earth Planet. Sci. Lett. 274, 423–438. https://doi.org/10.1016/j.epsl.2008.07.054

Wilkin, R.T., Barnes, H.L., 1997. Formation processes of framboidal pyrite. Geochim. Cosmochim. Acta 61, 323–339. https://doi.org/10.1016/S0016-7037(96)00320-1

Xu, Y., Yue, L., Jianxing, li, Sun, L., Sun, B., Zhang, J., Ma, J., Wang, J., 2009. An 11-Ma-old red clay sequence on the Eastern Chinese Loess Plateau. Palaeogeogr. Palaeoclimatol. Palaeoecol. - PALAEOGEOGR Palaeoclim. 284, 383–391. https://doi.org/10.1016/j.palaeo.2009.10.023

Yamazaki, T., Abdeldayem, A.L., Ikehara, K., 2003. Rock-magnetic changes with reduction diagenesis in Japan Sea sediments and preservation of geomagnetic secular variation in inclination during the last 30,000 years. Earth Planets Space 55, 327–340. https://doi.org/10.1186/BF03351766

Yao, Z., Shi, X., Guo, Z., Li, X., Nath, B.N., Betzler, C., Zhang, H., Lindhorst, S., Miriyala, P., 2023. Weakening of the South Asian summer monsoon linked to interhemispheric ice-sheet growth since 12 Ma. Nat. Commun. 14, 829. https://doi.org/10.1038/s41467-023-36537-6

Yu, Y., Notaro, M., Liu, Z., Wang, F., Alkolibi, F., Fadda, E., Bakhrjy, F., 2015. Climatic controls on the interannual to decadal variability in Saudi Arabian dust activity: Toward the development of a seasonal dust prediction model. J. Geophys. Res. Atmospheres 120, 1739–1758. https://doi.org/10.1002/2014JD022611

Zárate, M., Blasi, A., 1993. Late Pleistocene-Holocene eolian deposits of the southern Buenos Aires province, Argentina: A preliminary model. Quat. Int. 17, 15–20. https://doi.org/10.1016/1040-6182(93)90075-Q

Zembruscki, S.G., 1979. Geomorfologia da margem continental sul-brasileira e das bacias oceanicas adjacentes. In: Chaves, H.A.F. (Ed.), Geomorfologia da margem continental brasileira e das bacias oceanicas adjacentes, vol. 7. Petrobras, Rio de Janeiro, pp. 129-177.

Zhang, S., Qu, X., Huang, G., Hu, P., 2023. Asymmetric response of South Asian summer monsoon rainfall in a carbon dioxide removal scenario. Npj Clim. Atmospheric Sci. 6, 1–11. https://doi.org/10.1038/s41612-023-00338-x

Zhang, Z., Flatøy, F., Wang, H., Bethke, I., Bentsen, M., Guo, Z., 2012. Early Eocene Asian climate dominated by desert and steppe with limited monsoons. J. Asian Earth Sci. Complete, 24–35. https://doi.org/10.1016/j.jseaes.2011.05.013

Zheng, H., 2004. Late Miocene and mid-Pliocene enhancement of the East Asian monsoon as viewed from the land and sea. Glob. Planet. Change 41, 147–155. https://doi.org/10.1016/j.gloplacha.2004.01.003

Zheng, H., Wei, X., Tada, R., Clift, P.D., Wang, B., Jourdan, F., Wang, P., He, M., 2015. Late Oligocene–early Miocene birth of the Taklimakan Desert. Proc. Natl. Acad. Sci. 112, 7662–7667. https://doi.org/10.1073/pnas.1424487112

Zhisheng, A., Kutzbach, J.E., Prell, W.L., Porter, S.C., 2001. Evolution of Asian monsoons and phased uplift of the Himalaya-Tibetan plateau since Late Miocene times. Nature 411, 62–66. https://doi.org/10.1038/35075035

Zhou, J., Lau, K.-M., 1998. Does a Monsoon Climate Exist over South America? J. Clim. 11, 1020–1040. https://doi.org/10.1175/1520-0442(1998)011<1020:DAMCEO>2.0.CO;2

Zhuang, G., Pagani, M., Zhang, Y., 2017. Monsoonal upwelling in the western Arabian Sea since the middle Miocene. Geology 45, 655–658. https://doi.org/10.1130/G39013.1